Lipid bilayer dynamics from simultaneous analysis of orientation and frequency dependence of deuterium spin-lattice and quadrupolar order relaxation

Alexander A. Nevzorov, Theodore P. Trouard,* and Michael F. Brown†
Department of Chemistry, University of Arizona, Tucson, Arizona 85721
(Received 1 December 1997; revised manuscript received 10 April 1998)

Simultaneous analysis of the deuterium (^{2}H) NMR spin relaxation rates of lipid bilayers as a function of both frequency and sample orientation may be decisive in evaluating different models for the dynamics of membranes. Angular dependent ^{2}H spin-lattice (R_{1Z}) and quadrupolar order (R_{1Q}) ^{2}H relaxation rates have been measured at 46.1 and 76.8 MHz for macroscopically oriented bilayers of 1,2-diperdeuteriomyristoyl-*sn*-glycero-3-phosphocholine (DMPC-d_{54}), with perdeuterated acyl chains, in the liquid-crystalline (L_α) state. The data have been simultaneously fitted to various dynamical models, together with frequency dependent ^{2}H R_{1Z} data for vesicles of specifically ^{2}H-labeled DMPC. The same mechanism for the nuclear spin relaxation in lipids has been assumed for both oriented bilayers and vesicles, except for the presence of orientational averaging and a possible contribution from vesicle tumbling in the latter case. A noncollective model describing individual molecular reorientations in the presence of a potential of mean torque is able to adequately account for the orientation dependence; however, the quality of the fits to the frequency dispersion is less satisfactory. By contrast, a three-dimensional director fluctuation model accounts for the frequency dispersion for DMPC vesicles, but does not fit the orientation dependence of the R_{1Z} and R_{1Q} relaxation data. Higher-order director fluctuations have also been included, which do not significantly improve the quality of the fits to the collective model. Therefore, a composite membrane model is proposed including both noncollective molecular motions and director fluctuations. The model adequately describes both the frequency and orientation dependent data along the entire acyl chain simultaneously, which suggests that both dynamical processes can be detected by analyzing the ^{2}H NMR relaxation rates in the MHz range. Quantitative information about the bilayer dynamics including lipid reorientation rates, degree of molecular ordering, relative contributions from collective and noncollective motions, and director-frame spectral densities of motion has been obtained. The results suggest the bilayer dynamics in the MHz regime reflect molecular reorientations that are superimposed onto nematiclike deformations of the membrane interior in the liquid crystalline state.
[S1063-651X(98)10407-5]

PACS number(s): 87.22.Bt, 87.64.Hd, 76.60.−k

I. INTRODUCTION

Quantitative information about the dynamical and equilibrium properties of lipid bilayers, which comprise the essential structural matrix of biological membranes, can help establish a more definite picture about their material characteristics in relation to key biological processes in cells [1–4]. In most cases this information is embedded in various experimental observables, corresponding to interactions of various rank. Solid-state nuclear magnetic resonance (NMR) [5] spectroscopy provides a unique tool for studying such liquid-crystalline membrane assemblies. In the case of deuterium (^{2}H) NMR, lipid bilayers are investigated by isotopic substitution of deuterons for the protons of the lipid acyl chains, thus providing a nonperturbing probe of the equilibrium structure and dynamics as manifested in the second-rank quadrupolar interaction [6]. Here, the dynamics of the C—^{2}H bonds (segments), glycerol backbone, or polar head groups are related to fluctuations in the electric field gradient tensor, which give rise to the nuclear spin relaxation. Knowledge of the predominant mechanism for the ^{2}H NMR relaxation makes it possible to investigate such important bilayer properties as the elasticity, microviscosity, rotational diffusion coefficients, and correlation times for the various motions. These are contained in the theoretical spectral densities of motion, which can be derived for a particular model and fitted to the experimental spin relaxation rates by using NMR relaxation theory [7–11]. But despite the fact that lipid bilayers have been studied by ^{2}H NMR for a relatively long time [4,6,12–37], the predominant mechanism of the nuclear spin relaxation in these systems has not yet been revealed with certainty. One reason for this is that the angular dependence of the relaxation rates for oriented lipid bilayers in the liquid-crystalline state has been typically studied at a single magnetic field strength [18–20,22,23,26,28,33,34,38], whereas the frequency dispersion of the relaxation rates has been analyzed for the case of orientational averaging (vesicles and multilamellar dispersions) [15,16,21,27,37,39]. The results show that interpretations may differ depending on the type of the sample used, the number of fitting parameters in the model employed, or the viewpoints of particular investigators.

However, some general conclusions of a model-free nature can be deduced based on symmetry considerations alone [40]. For instance, the correlation functions and associated

*Present address: Department of Radiology, University of Arizona, Tucson, AZ 85724.
†Additional address: Division of Physical Chemistry 1, Center for Chemistry and Chemical Engineering, Lund University, S-221 00 Lund, Sweden.

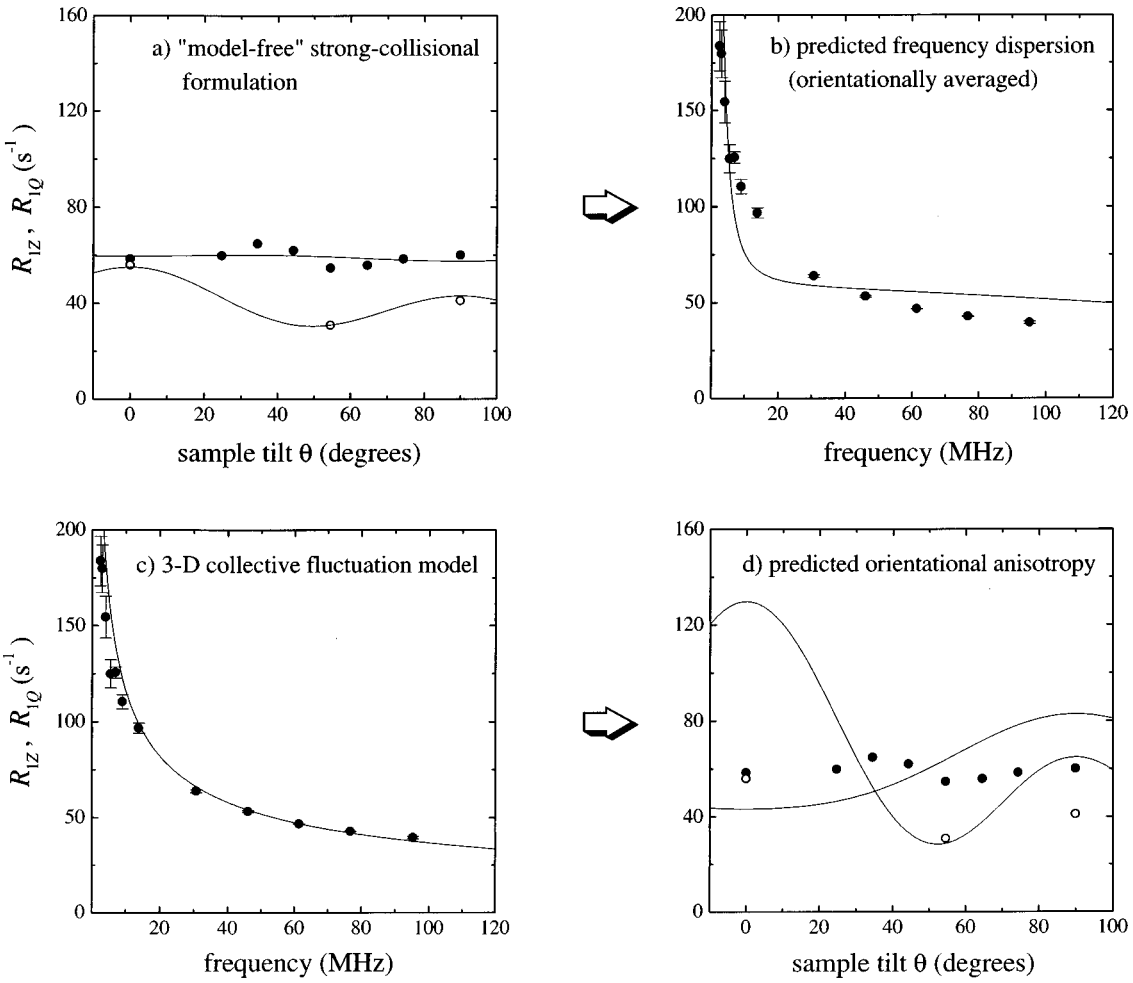

FIG. 1. Fits of ^{2}H R_{1Z} (●) and R_{1Q} (○) relaxation rates as a function of bilayer orientation [20] at 30.7 MHz for specifically deuterated 2 [4′,4′-$^2H_2$] DMPC, and as a function of frequency [27] for specifically deuterated 1,2 [3′,3′-$^2H_2$] DMPC vesicles in the liquid-crystalline state at $T=30$ °C. A simple ''model-free'' formulation for the rotational dynamics describes the orientational anisotropy, part (a), but fails to adequately predict the corresponding frequency dispersion, part (b), except near 30 MHz, i.e., the frequency at which the orientationally dependent data have been measured. By contrast, a 3D collective fluctuation model fits the frequency dependence, part (c), but does not account for the orientational dependence, part (d). Thus neither of the two treatments describes the nuclear spin relaxation of membrane lipid bilayers as a function of both frequency and sample orientation in terms of a single predominant mechanism (cf. the text).

spectral densities must be invariant to the symmetry operations of the point groups of both the molecule of interest and the phase. In the case of a lipid bilayer in the fluid (L_α) phase, one can assume that there is an effectively cylindrical symmetry about both the molecular long axis and the normal to the bilayer surface (director). This reduces the number of director-frame spectral densities for second-rank interactions to three, corresponding to projection indices of 0, 1, and 2 [39,41]. At a first level of approximation, the director-frame spectral densities can be treated in terms of a strong-collisional Markov process, without referring to a specific mechanism for the motion [38]. Under this relatively ''model-free'' assumption, each director-frame spectral density can be simply expressed in terms of the mean-squared fluctuation amplitude for a given rotation matrix element (projection index) and a single Lorentzian [34,38,42]. The mean-squared amplitudes and correlation times can then be regarded as independent fitting parameters, under the constraint that the corresponding order parameter can be determined experimentally from the quadrupolar splitting. As a specific illustration, part (a) of Fig. 1 shows fits of the above simple strong-collisional formulation to the orientation dependent ^{2}H spin-lattice (R_{1Z}) and quadrupolar order (R_{1Q}) ^{2}H relaxation rates measured at a single frequency (30.7 MHz) for macroscopically oriented bilayers of a representative lipid, 1,2-dimyristoyl-*sn*-glycero-3-phosphocholine (DMPC) [20]. Clearly the ''model-free'' theory [34,38] is able to describe adequately the orientational anisotropy of the relaxation. From the results of fitting the orientation dependent data, the corresponding frequency dispersion of the orientationally averaged ^{2}H R_{1Z} relaxation rates for lipid vesicles [27] can be predicted [Fig. 1 part (b)], which reveals a significant discrepancy with experiment. It follows that more detailed formulations may need to be considered, which take into account the molecular geometry and the specific type of motional processes, and yield relations among the correlation times for the various reorientational modes. More specific formulations that are successful in describing the orientational dependence, including jump models [18,22,23] and anisotropic continuous diffusion mod-

els [27,33,39,43], are also less adequate in their ability to fit the frequency dispersion of the relaxation [27,44]. Parts (c) and (d) of Fig. 1 show the opposite feature of an alternative model describing collective excitations of the bilayer in terms of elastic deformations treated as 3D director fluctuations [43,44]. In this case the model fits the frequency dispersion of the relaxation [16,27], but fails to adequately predict the orientational dependence [20]. Thus, none of the existing approaches, including the simple one-Lorentzian ''model-free'' approximation for each of the director-frame spectral densities, can describe the nuclear spin relaxation of membrane lipid bilayers as a function of *both* frequency and sample orientation in terms of a single mechanism.

In measuring the spin-lattice (R_{1Z}) or quadrupolar order (R_{1Q}) relaxation rates, only the laboratory-frame spectral densities are accessible, whereas it is the spectral densities in the frame of the normal to the bilayer surface (director) that are in principle most informative for a description of the lipid dynamics. By exploiting the transformation of the spectral densities to the laboratory frame and using NMR relaxation theory, it is possible to evaluate the director-frame spectral densities over an effectively twofold frequency range [45]. Fourier transformation of the director-frame spectral densities yields directly the correlation functions for the bilayer fluctuations [37], which can then be compared to molecular dynamics simulations. Only recently have measurements been reported in which the individual spectral densities of motion have been separated in the case of lipid bilayers [44,45], which has been also done for simpler liquid crystals [41,46,47]. For instance, Morrison and Bloom [34] have obtained director-frame spectral densities of motion corresponding to various acyl segments for lipid systems such as 1-perdeuteriopalmitoyl-2-oleoyl-*sn*-glycero-3-phosphocholine (POPC-d_{31}) and POPC-d_{31}:cholesterol without considering specific dynamical models in the manner described above. The spectral densities have been calculated directly from the orientational anisotropy of R_{1Z} and R_{1Q} relaxation rates at a single frequency (46.2 MHz) by using a general expression that separates the frequency dependence from the orientation dependence [42], as also outlined by Brown [38,43]. By determining a range for acceptable values of the fourth-rank order parameter, it has been argued that a discrete formulation for rotational chain isomerizations is inconsistent with the relaxation measurements. However, as noted above, such a ''model-independent'' formulation for the lipid dynamics may not be adequate for a description of the frequency dispersion, nor can any conclusions be made about the type of the dynamical mechanism predominant for the nuclear spin relaxation. Further interpretation of the relaxation data must therefore invoke detailed models. Moreover, the study of the frequency dependence of the relaxation especially at low-MHz frequencies is essential in order to distinguish between different dynamical models, since alternate formulations may describe the data as a function of a single variable equally well [34].

A comprehensive dynamical model aimed at describing the predominant mechanisms for the nuclear spin relaxation of lipid bilayers should account *simultaneously* for the orientation dependence of the relaxation rates as a function of frequency with the same values of the fitting parameters. In the present work an extensive body of experimental data has been analyzed, involving the orientational anisotropy of the ^{2}H R_{1Z} and R_{1Q} relaxation rates measured at 46.1 and 76.8 MHz for 1,2-diperdeuteriomyristoyl-*sn*-glycero-3-phosphocholine (DMPC-d_{54}) in the liquid crystalline (L_α) state, having perdeuterated acyl chains, together with the ^{2}H R_{1Z} frequency dispersion for vesicles of DMPC with specifically ^{2}H-labeled acyl chains [27,44]. Various dynamical models, which take into account collective and noncollective motions of lipids within the bilayer, have been fitted to the data. The models have been tested for their ability to fit simultaneously the relaxation rate anisotropy for oriented multilamellar dispersions and the frequency dispersion for lipid vesicles in the presence of orientational averaging. These findings suggest that collective excitations of lipid bilayers together with molecular rotations may influence the orientation and frequency dependence of the ^{2}H NMR relaxation in the mid-MHz range.

II. DYNAMICS AND NUCLEAR SPIN RELAXATION

NMR relaxation theory considers the behavior of a spin probe in the presence of a randomly fluctuating time-dependent perturbation of the Zeeman Hamiltonian, which corresponds to various tensorial interactions. In the case of ^{2}H NMR spectroscopy, the perturbing quadrupolar interaction depends on the orientation of the principal axes of the second-rank electric field gradient (EFG) tensor that is associated with a particular C—^{2}H bond (segment) relative to the main magnetic field (laboratory frame). Fluctuations of the EFG tensor in a lipid bilayer relative to the laboratory frame can be due in general to a combination of fast segmental motions, noncollective molecular reorientations, and collective excitations of the bilayer formulated as director fluctuations [44]. In terms of an irreducible representation for the second-rank interactions [4,36,48], the correlation functions describing the overall time-dependent orientation of the coupling tensor with respect to the laboratory frame are expressed in terms of the components of the second-rank Wigner rotation matrix $\mathbf{D}^{(2)}(\Omega_{PL})$, that is to say

$$G_m(\tau,\beta_{DL}) = \langle [D^{(2)}_{0m}(\Omega_{PL};t+\tau) - \langle D^{(2)}_{0m}(\Omega_{PL})\rangle]^* \times [D^{(2)}_{0m}(\Omega_{PL};t) - \langle D^{(2)}_{0m}(\Omega_{PL})\rangle]\rangle, \quad (2.1)$$

where $m=0$, ± 1, or ± 2 is the projection index, and the elements of the Wigner rotation matrix are tabulated elsewhere [4]. Note that only a single index m is retained in the above notation for the correlation function, corresponding to an axially symmetric static EFG coupling tensor in the case of the quadrupolar interaction. The angle $\beta_{DL} \equiv \theta$ denotes the tilt of the specimen (average director), about which there is cylindrical symmetry, with respect to the external magnetic field; whereas the overall Euler angles Ω_{PL} describe the time-dependent orientation of the principal axis system (PAS) associated with the C—^{2}H bond relative to the main magnetic field. Here we use the Rose [49] convention for body-fixed right-handed rotations together with the Rose [49] convention for the Wigner rotation matrices.

The spectral densities of motion $J_m(\omega,\beta_{DL})$ in the laboratory frame are defined by Fourier transformation of the above correlation functions,

$$J_m(\omega,\beta_{DL})=\int_{-\infty}^{+\infty}G_m(\tau,\beta_{DL})e^{-i\omega\tau}d\tau. \tag{2.2}$$

To separate the frequency dependence of the laboratory-frame spectral densities $J_m(\omega,\beta_{DL})$ from their orientation dependence, one can expand the overall transformation of the EFG tensor to the laboratory frame by using the closure property of the Wigner rotation matrices [4,50], leading to

$$D^{(2)}_{0m}(\Omega_{PL};t)=\sum_{p=-2}^{2}D^{(2)}_{0p}(\Omega_{PD};t)D^{(2)}_{pm}(\Omega_{DL}). \tag{2.3}$$

The Euler angles $\Omega_{PD}(t)$ transform the EFG coupling tensor to the frame associated with the average director and contain the time dependence; whereas the angles Ω_{DL} describe the static orientation of the sample with respect to the laboratory frame. Substituting Eq. (2.3) into Eq. (2.1) and Fourier transforming, the relation between the spectral densities in the laboratory frame and the frame of the bilayer normal (director), in the case of axially symmetric molecules and an axially symmetric distribution about the director axis, can be written as [39,41]

$$\begin{aligned}J_m(\omega,\beta_{DL})=&\,d^{(2)}_{0m}(\beta_{DL})^2J^{\rm dir}_0(\omega)\\&+[d^{(2)}_{-1m}(\beta_{DL})^2+d^{(2)}_{1m}(\beta_{DL})^2]J^{\rm dir}_1(\omega)\\&+[d^{(2)}_{-2m}(\beta_{DL})^2+d^{(2)}_{2m}(\beta_{DL})^2]J^{\rm dir}_2(\omega).\end{aligned} \tag{2.4}$$

In the above general expression ω is the angular frequency and β_{DL} is the angle at which the sample is tilted relative to the main magnetic field. Only the reduced Wigner matrix elements $d^{(2)}_{nm}(\beta_{DL})$, where n, $m=0$, ±1, and ±2, are retained to emphasize the angular dependence solely on β_{DL}. The director-frame spectral densities $J^{\rm dir}_p(\omega)$, where $p=0$, 1, 2, are given by

$$\begin{aligned}J^{\rm dir}_p(\omega)=\int_{-\infty}^{\infty}&\langle[D^{(2)}_{0p}(\Omega_{PD};t+\tau)-\langle D^{(2)}_{0p}(\Omega_{PD})\rangle]^*\\&\times[D^{(2)}_{0p}(\Omega_{PD};t)-\langle D^{(2)}_{0p}(\Omega_{PD})\rangle]\rangle e^{-i\omega\tau}d\tau.\end{aligned} \tag{2.5}$$

Here the symmetry property of the reduced Wigner matrix elements, i.e., $d^{(2)}_{0p}(\beta_{PD};t)=(-1)^pd^{(2)}_{0-p}(\beta_{PD};t)$, has been used, leading to three different values of the director-frame spectral densities. Equation (2.4) can be further rewritten in terms of even-rank Legendre polynomials $P_j(\cos\beta_{DL})$, where $j=0$, 2, and 4, by using the Clebsch-Gordan series expansion as discussed in detail by Brown [43] and Trouard *et al.* [33,51]. This yields the following general orientational dependence of the laboratory-frame spectral densities, cf. also Morrison and Bloom [34],

$$\begin{aligned}J_m(\omega,\beta_{DL})=&\sum_{p=0,1,2}\;\sum_{j=0,2,4}(2-\delta_{p0})c^{(j)}_pc^{(j)}_m\\&\times P_j(\cos\,\beta_{DL})J^{\rm dir}_p(\omega),\end{aligned} \tag{2.6}$$

where the coefficients $c^{(j)}_p$ and $c^{(j)}_m$ are related to the Wigner $3-j$ symbols [33].

It should be emphasized that at this level the analysis is relatively model free, apart from the assumption of a stationary Markov process and the specific symmetry of the problem corresponding to the molecular structure as well as the phase of interest. Therefore, any model-dependent assumptions are contained in the interpretation of the director-frame spectral densities. For example, in the case of a strong-collisional approximation, the latter can be written in terms of mean-squared amplitudes and reduced spectral densities [38,43] as

$$\begin{aligned}J^{\rm dir}_p(\omega)=&[\langle|D^{(2)}_{0p}(\Omega_{PD})|^2\rangle\\&-|\langle D^{(2)}_{0p}(\Omega_{PD})\rangle|^2\delta_{0p}j^{(2)}_{0p}(\Omega_{PD};\omega),\end{aligned} \tag{2.7}$$

where the reduced spectral densities $j^{(2)}_{0p}(\Omega_{PD};\omega)$ are Lorentzians with correlation times τ_p. Note that Eq. (2.7) does not refer to any specific type of motion, nor the orientation of the coupling tensor with respect to the long molecular axis; the latter can result in a spectrum of correlation times for the overall director-frame spectral density $J^{\rm dir}_p(\omega)$ rather than a single correlation time τ_p (*vide infra*). Despite its ''model-independent'' features, Eq. (2.7) is probably not suitable for a description of the membrane dynamics as it does not adequately predict the experimentally observed orientationally averaged frequency dispersion; cf. Fig. 1. This may indicate the presence of a more complex motional process that cannot be described by a single-Lorentzian approximation for each of the three director-frame spectral densities.

In terms of the laboratory-frame spectral densities of motion, for the specific case of the quadrupolar interaction, the spin-lattice relaxation rate is given by [9,36]

$$R_{1Z}(^2{\rm H})=\tfrac{3}{4}\pi^2\chi_Q^2[J_1(\omega_{\rm D},\beta_{DL})+4J_2(2\omega_{\rm D},\beta_{DL})]. \tag{2.8}$$

Here $\chi_Q=e^2qQ/h=170$ kHz is the static quadrupolar coupling constant, and $\omega_{\rm D}$ is the deuteron Larmor frequency. Similarly, the relaxation of the quadrupolar order of the quadrupolar interaction, i.e., relaxation of the quantity $\langle 3\hat{I}_z^2-I(I+1)\rangle$, is given by [36]

$$R_{1Q}(^2{\rm H})=\tfrac{9}{4}\pi^2\chi_Q^2J_1(\omega_{\rm D},\beta_{DL}). \tag{2.9}$$

The nuclear spin relaxation rates as given by Eqs. (2.8) and (2.9) contain not only the frequency dependence (ω), but also the dependence on the macroscopic orientation of the bilayer with respect to the magnetic field (laboratory frame) (β_{DL}), cf. Eqs (2.4) and (2.6). In the case of macroscopically oriented bilayers, only the laboratory-frame spectral densities can be obtained by using Eqs. (2.8) and (2.9), and further calculation of the director-frame spectral densities is needed, as given by Eqs. (2.4) and (2.6). Note that in the case of multilamellar dispersions [15] and vesicles [14], the angular anisotropy is averaged over all possible orientations. Consequently, in order to fit simultaneously both the R_{1Z} and R_{1Q} angular anisotropies at different frequencies, the functional form of $J_m(\omega,\beta_{DL})$ must be derived from a physical model describing the motion of a particular C—^{2}H bond (segment).

III. NONCOLLECTIVE AND COLLECTIVE MODELS FOR MEMBRANE DYNAMICS

Depending on the choice of the model, the spectral densities of motion $J_m(\omega,\beta_{DL})$ can be calculated, for which the common feature is a decomposition of the overall transformation of the EFG tensor from the principal axis system to the laboratory frame into various subtransformations [44]. The spectral densities take into account the geometry and the complicated character of the motions of the bilayer components, as well as the macroscopic orientation of the sample as a whole relative to the main magnetic field.

A. Local fast motions

Continuous segmental motions. By introducing an additional subtransformation from the PAS to the intermediate segmental frame given by the Euler angles Ω_{PI}, the ''model-free'' strong-collisional approximation [38], Eqs. (2.4) and (2.7), can be generalized as [33,44]

$$J_m(\omega,\beta_{DL})=\sum_r\sum_n\left|D^{(2)}_{0r}(\Omega_{PI})-\frac{\eta_Q}{\sqrt{6}}[D^{(2)}_{-2r}(\Omega_{PI})+D^{(2)}_{2r}(\Omega_{PI})]\right|^2 \times[\langle|D^{(2)}_{rn}(\Omega_{ID})|^2\rangle-|\langle D^{(2)}_{rn}(\Omega_{ID})\rangle|^2\delta_{r0}\delta_{n0}]j^{(2)}_{rn}(\Omega_{ID};\omega)|D^{(2)}_{nm}(\Omega_{DL})|^2, \tag{3.1}$$

where angles Ω_{ID} pertain to the time-dependent orientation of the segmental frame with respect to the frame of the bilayer director, and Ω_{DL} describe the sample tilt relative to the main magnetic field (laboratory frame). One approach is to consider random segmental reorientations, e.g., arising from rotational isomerizations of the acyl chains approximated as continuous diffusion. The reduced spectral densities $j^{(2)}_{rn}(\Omega_{ID};\omega)$ can then be treated in terms of continuous angular diffusion in the presence of a potential of mean torque, referred to as the segmental diffusion model (model I) [37,43,44]. As shown elsewhere [27,37,44], the segmental diffusion model (I) does not fit the frequency dispersion of the ^{2}H and ^{13}C R_{1Z} relaxation rates for randomly oriented samples in the MHz regime and, therefore, it will not be further considered here.

Discrete local jumps. As an alternative, random segmental or molecular reorientations can be treated in terms of discrete jumps [23,52,53] for which the ''model-free'' Eq. (2.4) should be modified to account for the nondiagonal terms [52]. In the case of nearest-neighbor jumps among N equivalent sites on the rim of a cone, the following result is obtained [52]:

$$J_m(\omega,\beta_{DL})=\sum_{n'\neq 0}\sum_{n\neq 0}|D^{(2)}_{0n'}(\Omega_{PD})^*D^{(2)}_{0n}(\Omega_{PD})| \times j^{(2)}_{n'n}(\gamma_{PD};\omega)D^{(2)}_{n'm}(\Omega_{DL})^*D^{(2)}_{nm}(\Omega_{DL}), \tag{3.2}$$

where $\Omega_{PD}=[0,\beta_{PD},\gamma_{PD}(0)]$. In the above formula $j^{(2)}_{n'n}(\gamma_{PD};\omega)$ are Lorentzians with correlation times given by [52]

$$\frac{1}{\tau_{n'n}}=4k\,\sin^2\left(\frac{\pi n}{N}\right), \tag{3.3}$$

in which k is the jump rate and $n=n'\ (\mathrm{mod}\ N)$. In the case of three-site jumps, the model predicts a single correlation time $1/\tau_{n'n}\rightarrow 1/\tau=3k$, as given by Eq. (3.3). However, it has been shown in earlier work [44] that spectral densities with a single correlation time do not fit the experimental frequency dispersion for vesicles and multilamellar dispersions. Moreover, relatively short correlation times for the segmental or molecular jumps, which occur on the subnanosecond time scale [23], would result in little or no frequency dependence of the ^{2}H R_{1Z} relaxation rates within the MHz range (extreme narrowing limit). A pronounced frequency dispersion is observed in the case of vesicles and multilamellar dispersions [15,16,27]. Consequently it seems doubtful whether a jump model alone can account for the experimental frequency behavior of the ^{2}H R_{1Z} relaxation rates of bilayer lipids in the fluid state within the entire MHz range.

Other approaches for calculating correlation functions for fast motions of the lipid constituents can also be considered. These included more detailed treatments of the internal lipid chain dynamics [54,55], models involving the stochastic Liouville–von Neumann equation [29,56], as well as Brownian [57], Langevin [58], and molecular dynamics (MD) simulations [59–63]. In the above cases rapid local motions of the lipids are primarily investigated, which may be superimposed on slower molecular or collective reorientations (*vide infra*).

B. Slow order fluctuations

In addition, one can consider formulations for slower membrane motions, which specifically encompass noncollective molecular reorientations (model II) [33,39,43], and models for collective order fluctuations. The latter can be formulated either as two-dimensional (2D) thermal excitations (model III) [64,65], or three-dimensional (3D) excitations (model IV) [43,66,67]. As shown earlier [27,37,44,68], a 2D director fluctuation model (III) does not account for the frequency dispersion of ^{2}H and ^{13}C R_{1Z} relaxation rates for randomly oriented samples in the MHz regime, and thus it will not be further discussed here. Hence the treatments we consider for describing the slow motions of membrane constituents, which may govern the spin relaxation in the ^{2}H NMR MHz range, include the molecular rotational diffusion model (model II) and a membrane deformation model in-

volving a continuous spectrum of three-dimensional director fluctuations (model IV) [43,66,69,70].

Molecular motions. The molecular order fluctuations include the preaveraging of the coupling tensor left over from faster segmental motions (time-scale separation and statistical independence are assumed) and involve four subtransformations. The first set of Euler angles Ω_{PI} transforms the *static* EFG tensor from the PAS to the intermediate frame (averaged with respect to the faster segmental motions), in which the residual EFG tensor is *diagonal*; the second fixed set Ω_{IM} pertains to the transformation of the *residual* EFG tensor to the molecular frame; the third set $\Omega_{MD}(t)$ corresponds to the time-dependent orientation of the molecule with respect to the bilayer normal (director); and finally, Ω_{DL} performs the fourth transformation from the fixed director frame to the laboratory frame. The ''model-free'' expression for the spectral density, Eq. (2.4), can then be generalized to account for the pre-averaging due to local fast motions in the following way [33,43,44]:

$$J_m(\omega,\beta_{DL})=|\langle D_{00}^{(2)}(\Omega_{PI})\rangle|^2\sum_q\sum_n\left|D_{0q}^{(2)}(\Omega_{IM})-\frac{\eta_Q^{\rm eff}}{\sqrt{6}}\left[D_{-2q}^{(2)}(\Omega_{IM})+D_{2q}^{(2)}(\Omega_{IM})\right]\right|^2$$
$$\times[\langle|D_{qn}^{(2)}(\Omega_{MD})|^2\rangle-|\langle D_{qn}^{(2)}(\Omega_{MD})\rangle|^2\delta_{q0}\delta_{n0}]j_{qn}^{(2)}(\Omega_{MD};\omega)|D_{nm}^{(2)}(\Omega_{DL})|^2. \quad (3.4)$$

Here $\eta_Q^{\rm eff}$ is the effective asymmetry parameter of the residual EFG tensor, which is modulated by the faster segmental motions [33,71]. Correlation times for the Lorentzian reduced spectral densities $j_{qn}^{(2)}(\Omega_{MD};\omega)$ can be found by treating the molecular reorientations as angular diffusion in the presence of a potential of mean torque [33,72,73], which yields

$$\frac{1}{\tau_{qn}}=\frac{\mu_{qn}}{\langle d_{qn}^{(2)}(\beta_{MD})^2\rangle-\langle d_{qn}^{(2)}(\beta_{MD})\rangle^2\delta_{q0}\delta_{n0}}D_\perp+(D_\parallel-D_\perp)n^2, \quad (3.5)$$

where $d_{qn}^{(2)}(\beta_{MD})$ are the reduced Wigner matrix elements. The moments μ_{qn} can be evaluated in terms of the order parameters $\langle d_{00}^{(j)}(\beta_{MD})\rangle$, $j=1,2,3,4$ by using the Clebsch-Gordan series expansion as discussed by Trouard *et al.* [33]. These, in turn, can be found from the Boltzmann distribution in terms of the potential of mean torque $U(\beta_{MD})$,

$$\langle d_{00}^{(j)}(\beta_{MD})\rangle=\frac{\int_0^\pi d_{00}^{(j)}(\beta_{MD})\exp[-U(\beta_{MD})/kT]\sin\beta_{MD}d\beta_{MD}}{\int_0^\pi\exp[-U(\beta_{MD})/kT]\sin\beta_{MD}d\beta_{MD}}. \quad (3.6)$$

The potential $U(\beta_{MD})$ can be chosen as $U(\beta_{MD})=-\lambda_jP_j(\cos\beta_{MD})$, where $P_j(\cos\beta_{MD})$ is a Legendre polynomial [74]. For $j=1$ one has an odd parity with respect to the inversion $\beta_{MD}\rightarrow\pi-\beta_{MD}$; whereas for $j=2$ the parity is even. Assuming $\eta_Q^{\rm eff}=0$, the amplitudes of fast segmental motions $\langle D_{00}^{(2)}(\Omega_{PI})\rangle$ in Eq. (3.4) can be expressed in terms of the order parameter $S_{\rm CD}=\langle D_{00}^{(2)}(\Omega_{PI})\rangle D_{00}^{(2)}(\Omega_{IM})\langle D_{00}^{(2)}(\Omega_{MD})\rangle$, which is experimentally determined from the ^{2}H NMR quadrupolar splitting for a given sample orientation, namely, $\Delta\nu_Q=\frac{3}{2}\chi_QS_{\rm CD}D_{00}^{(2)}(\Omega_{DL})$. According to Eqs. (2.8), (2.9), and (3.4), for a given segmental position i the ^{2}H $R_{1Z}^{(i)}$ and $R_{1Q}^{(i)}$ relaxation rates should then be proportional to the corresponding order parameter $S_{\rm CD}^{(i)}$ squared [75]. Note that the above result in the limit of $\eta_Q^{\rm eff}=0$ is applicable to both the methylene groups of the acyl chain as well as the chain terminal methyl groups. In the latter case the threefold rotation leads to a reduction of the quadrupolar coupling [76] by a factor of $-1/3$. This can be included in the spectral densities $J_m(\omega,\beta_{DL})$ in terms of the fast order parameter $S_f^{(2)}\equiv\langle D_{00}^{(2)}(\Omega_{PI})\rangle$. By contrast, the relaxation rates as given by the simple ''model-free'' strong-collisional formulation, Eq. (2.7), segmental diffusion model (I), Eq. (3.1), or by a jump model, Eq. (3.2), do not contain such a square-law dependence on the order parameter. This important issue will be discussed further in the text.

Collective membrane excitations. An alternative to the molecular diffusion model (II) is to consider order fluctuations due to collective membrane excitations, in which the bilayer is considered as a continuous medium [43]. Several models have been proposed to treat such collective excitations in terms of deformations of a smecticlike liquid crystal [65,69,77,78]. In a recent contribution [78] the various regimes of bilayer couplings have been theoretically investigated, which are predicted to influence the ^{2}H NMR relaxation at frequencies much lower than the MHz regime. However, in the present paper we analyze the ^{2}H relaxation rates measured at frequencies of 2.5 MHz and higher, which may correspond to essentially uncoupled membrane deformations [44]. If one considers small fluctuations in linear order, a model for collective director fluctuations gives the following result for the spectral densities [44],

$$J_m(\omega,\beta_{DL})=\tfrac{5}{2}|\langle D_{00}^{(2)}(\Omega_{PN})\rangle|^2D\omega^{-(2-d/2)}\times[|D_{-1m}^{(2)}(\Omega_{DL})|^2+|D_{1m}^{(2)}(\Omega_{DL})|^2]. \quad (3.7)$$

Here the constant factor D is a function of the elasticity, viscosity, and temperature of the bilayer, and d is the dimensionality of the thermal excitations. The first rotation from

the PAS of the coupling tensor to the frame of the instantaneous bilayer normal (director) is defined by the Euler angles Ω_{PN}, and the second transformation to the frame of the average director is given by Ω_{ND}, so that the observed order parameter for small-amplitude fluctuations can be written as $S_{\mathrm{CD}}=\langle D_{00}^{(2)}(\Omega_{PN})\rangle\langle D_{00}^{(2)}(\Omega_{ND})\rangle$. In this case a square-law functional dependence of the ^{2}H $R_{1Z}^{(i)}$ and $R_{1Q}^{(i)}$ relaxation rates on the order parameter $S_{\mathrm{CD}}^{(i)}$ is predicted by the model for the entire chain including both the methylene and methyl groups as discussed above. It has been shown in previous work [16,27,37,44,68] that only the case of $d=3$ accounts for the frequency dispersion of the relaxation rates for phospholipid vesicles (model IV) in the MHz range, whereas at much lower frequencies other regimes including $d=2$, may influence the relaxation [21,29,78].

Formulations of the director fluctuations up to quadratic order have been also proposed [70,79] for the case of $d=3$, yielding the following expression [70]:

$$J_m(\omega,\beta_{DL})=\frac{3\pi}{4}\frac{S_{\mathrm{CD}}^2}{S_s^{(2)^2}}\left\{\frac{3(\lambda/kT)^2}{\omega_c}\ln\left[1+\left(\frac{\omega_c}{\omega}\right)^2\right]|D_{0m}^{(2)}(\Omega_{DL})|^2+\frac{4(\lambda/kT)}{\sqrt{2\omega_c}}\frac{1}{\sqrt{\omega}}u\left(\frac{\omega}{\omega_c}\right)[|D_{-1m}^{(2)}(\Omega_{DL})|^2\right.$$
$$\left.+|D_{1m}^{(2)}(\Omega_{DL})|^2]+\frac{(\lambda/kT)^2}{\omega_c}\ln\left[1+\left(\frac{\omega_c}{\omega}\right)^2\right][|D_{-2m}^{(2)}(\Omega_{DL})|^2+|D_{2m}^{(2)}(\Omega_{DL})|^2]\right\}. \tag{3.8}$$

In the above expression $\lambda/kT=kTq_c/2\pi^2K$, and $\omega_c=Kq_c^2/\eta$ is the cutoff frequency, where K designates the macroscopic elastic constant for the bilayer, η is the bilayer viscosity, and q_c is the upper cutoff for the director excitation modes. The slow order parameter is given [70] by $S_s^{(2)}=1-3\lambda/kT$ and the cutoff function $u(x)$ is [80]

$$u(x)=1+\frac{1}{2\pi}\ln\left(\frac{1-\sqrt{2x}+x}{1+\sqrt{2x}+x}\right)-\frac{1}{\pi}\tan^{-1}\left(\frac{\sqrt{2x}}{1-x}\right), \tag{3.9}$$

where $x\equiv\omega/\omega_c<1$. Note that in comparison with Eq. (3.7), which takes into account only linear-order director fluctuations, Eq. (3.8) includes additional terms containing $D_{0m}^{(2)}(\Omega_{DL})$ and $D_{\pm2m}^{(2)}(\Omega_{DL})$ that also influence the dependence on the sample tilt angle β_{DL}. Equation (3.8) also predicts the square-law dependence on the observed order parameter S_{CD}, and the second term of Eq. (3.8) linear in λ/kT yields Eq. (3.7) as a limiting case if $\omega\ll\omega_c$. The effect of these higher-order terms on the nuclear spin relaxation of lipid bilayers will be discussed later.

IV. COMPOSITE MODEL FOR NONCOLLECTIVE AND COLLECTIVE MOTIONS

It is also possible that various types of motional processes occur simultaneously in the lipid bilayer, including faster segmental motions, molecular reorientations, and collective director fluctuations. An alternative to the previous models, which consider these processes separately, involves a composite statistical model that accounts for the various motions simultaneously. Existing methods for calculating the correlation function (spectral density) for a composite motional process include either a simple summation of the correlation functions corresponding to the individual motions [21,33,39,43], i.e., by assuming their statistical independence and time-scale separation, or additional consideration of cross correlations [80]. Perhaps the most rigorous approach is to solve directly the density matrix equation in the presence of a generalized Markov operator acting on the various stochastic variables [56] instead of using Eqs. (2.8) and (2.9).

Here we further apply the convenient closure property of the Wigner rotation matrices [50] and, following Ukleja *et al.* [67], combine the membrane deformation model (3D director fluctuations; model IV) with a model for molecular reorientations in the presence of a potential of mean torque [72]. We assume that the faster segmental motions occur on a short time scale compared to the ^{2}H NMR frequency range, so that we keep the preaveraged segmental amplitudes $\langle D_{00}^{(2)}(\Omega_{PI})\rangle$ as in Eq. (3.4). One can then include in the overall transformation of the coupling tensor $D_{0m}^{(2)}(\Omega_{PL})$ an additional time-dependent subtransformation $D_{np}^{(2)}(\Omega_{ND};t)$ describing fluctuations of the instantaneous membrane normal (director) with respect to its average position,

$$D_{0m}^{(2)}(\Omega_{PL})=\langle D_{00}^{(2)}(\Omega_{PI})\rangle\sum_q\sum_n\sum_p D_{0q}^{(2)}(\Omega_{IM})$$
$$\times D_{qn}^{(2)}(\Omega_{MN};t)D_{np}^{(2)}(\Omega_{ND};t)D_{pm}^{(2)}(\Omega_{DL}). \tag{4.1}$$

Here the Euler angles $\Omega_{MN}(t)$ describe the time-dependent orientation of the molecule with respect to the instantaneous normal to the bilayer surface (director), and the angles $\Omega_{ND}(t)$ pertain to the time-dependent orientation of the instantaneous director with respect to the average director, thus manifesting the effect of collective motions. The possible correlations between the noncollective molecular motions and the collective director fluctuations are neglected for simplicity, which does not necessarily presuppose their time-scale separation. Due to this assumption, one can average over these motions separately. We also suggest that the average orientation of the z axis of the intermediate frame for the residual EFG tensor as a result of the segmental fluctuations is nearly perpendicular to the long molecular axis [44], so that $\beta_{IM}=90°$.

Using Eqs. (2.1) and (4.1) one can then write for the director-frame correlation functions that

$$G_p^{\mathrm{dir}}(\tau)=\frac{S_{\mathrm{CD}}^2}{S_s^{(2)^2}}\sum_{n=-2}^{2}\left\{[G_{0n}^{\mathrm{mol}}(\tau)+S_s^{(2)^2}\delta_{0n}]G_{np}^{\mathrm{col}}(\tau)+\frac{3}{2}[G_{-2n}^{\mathrm{mol}}(\tau)+G_{2n}^{\mathrm{mol}}(\tau)]G_{np}^{\mathrm{col}}(\tau)-S_s^{(2)^2}\delta_{0n}\delta_{0p}\right\},\tag{4.2}$$

where the slow order parameter is $S_s^{(2)}=\langle D_{00}^{(2)}(\Omega_{MN})\rangle\langle D_{00}^{(2)}(\Omega_{ND})\rangle\approx\langle D_{00}^{(2)}(\Omega_{MN})\rangle$ for small-amplitude director fluctuations, and $p=0,1,2$. The director-frame correlation functions for noncollective molecular motions are given by

$$G_{qn}^{\mathrm{mol}}(\tau)=[\langle|D_{qn}^{(2)}(\Omega_{MN})|^2\rangle-|\langle D_{qn}^{(2)}(\Omega_{MN})\rangle|^2\delta_{q0}\delta_{n0}]e^{-t/\tau_{qn}},\tag{4.3}$$

in which $q=0,\pm2$ and τ_{qn} are given by Eq. (3.5). Taking into account only the director fluctuations to linear order in $\beta_{ND}(t)$ [43,81], one can further write that

$$G_{00}^{\mathrm{col}}(\tau)=G_{11}^{\mathrm{col}}(\tau)=G_{22}^{\mathrm{col}}(\tau)=1,\tag{4.4a}$$

$$G_{12}^{\mathrm{col}}(\tau)=G_{21}^{\mathrm{col}}(\tau)=\langle\beta_{ND}(t+\tau)\beta_{ND}(t)\rangle\equiv g^{\mathrm{col}}(\tau),\tag{4.4b}$$

$$G_{01}^{\mathrm{col}}(\tau)=G_{\pm10}^{\mathrm{col}}(\tau)=\tfrac{3}{2}g^{\mathrm{col}}(\tau).\tag{4.4c}$$

All other collective correlation functions for q and n that appear in Eq. (4.2) are zero in this order. The *reduced* collective director-frame correlation function $g^{\mathrm{col}}(\tau)$ corresponds to Eq. (3.7) under the assumption of an infinite upper limit for the excitation modes, and is

$$g^{\mathrm{col}}(\tau)=\frac{5}{3\sqrt{2\pi}}\frac{D}{\sqrt{\tau}}.\tag{4.5}$$

From Eqs. (4.2)–(4.5) and inverse Fourier transforming to the frequency domain, one finally obtains for the overall spectral density, referred to herein as the composite membrane deformation model (V), that [11,67]

$$J_m(\omega,\beta_{DL})=J_m^{\mathrm{mol}}(\omega,\beta_{DL})+J_m^{\mathrm{col}}(\omega,\beta_{DL})+J_m^{\text{mol-col}}(\omega,\beta_{DL}),\tag{4.6}$$

where $J_m^{\mathrm{mol}}(\omega,\beta_{DL})$ is given by the molecular diffusion model (II), Eq. (3.4), and $J_m^{\mathrm{col}}(\omega,\beta_{DL})$ corresponds to small-amplitude 3D collective fluctuations (model IV), Eq. (3.7). The cross-term $J_m^{\text{mol-col}}(\omega,\beta_{DL})$ is equal to

$$J_m^{\text{mol-col}}(\omega,\beta_{DL})=\frac{S_{\mathrm{CD}}^2}{S_s^{(2)^2}}\left\{J_{01}^{\text{mol-col}}(\omega)+\frac{3}{2}[J_{-21}^{\text{mol-col}}(\omega)+J_{21}^{\text{mol-col}}(\omega)]\right\}[3d_{0m}^{(2)}(\beta_{DL})^2+d_{-2m}^{(2)}(\beta_{DL})^2+d_{2m}^{(2)}(\beta_{DL})^2]+\left\{J_{02}^{\text{mol-col}}(\omega)+\frac{3}{2}[J_{-22}^{\text{mol-col}}(\omega)+J_{22}^{\text{mol-col}}(\omega)]+\frac{3}{2}[J_{00}^{\text{mol-col}}(\omega)+3J_{20}^{\text{mol-col}}(\omega)]\right\}\times[d_{-1m}^{(2)}(\beta_{DL})^2+d_{1m}^{(2)}(\beta_{DL})^2].\tag{4.7}$$

It is noteworthy that since the above cross-term has originated from Eqs. (4.1) and (4.2), which correspond to the transformation properties of the coupling tensor, it is purely geometrical and does not reflect any correlations between the molecular motions and director fluctuations (statistical dependence). In the linear-order approximation for director amplitudes, the individual terms $J_{qn}^{\text{mol-col}}(\omega)$ contain Fourier transforms of the products of the correlation functions corresponding to the various modes of molecular reorientations q and n, and the reduced correlation function for collective motions $g^{\mathrm{col}}(\tau)$, Eq. (4.5). By calculating the Fourier integrals one obtains, cf. Ukleja *et al.* [67],

$$J_{qn}^{\text{mol-col}}(\omega)=[\langle|D_{qn}^{(2)}(\Omega_{MN})|^2\rangle-|\langle D_{qn}^{(2)}(\Omega_{MN})\rangle|^2\delta_{q0}\delta_{n0}]\frac{5}{3}D\sqrt{\frac{\tau_{qn}[1+\sqrt{1+(\omega\tau_{qn})^2}]}{1+(\omega\tau_{qn})^2}},\tag{4.8}$$

for all q and n that appear in Eq. (4.7). Note also that for this model both the pure terms corresponding to noncollective and collective motions, as well as the cross-term yield a square-law dependence of the relaxation rates on the order parameter S_{CD}.

V. MATERIALS AND METHODS

Phospholipid synthesis and preparation of oriented samples. The synthesis of DMPC-d_{54}, having two perdeuterated acyl chains, was carried out from the cadmium adduct

of *sn*-glycero-3-phosphocholine and the anhydride of perdeuterated myristic acid [82,83]. We prepared perdeuterated myristic acid by catalytic exchange of deuterium for hydrogen over a 10% Pd-charcoal catalyst (Aldrich, Milwaukee, WI) at 195 °C using ^2H gas generated electrolytically from ^2H_2O (99.8 at. %; Aldrich, Milwaukee, WI). The incorporation of ^2H and the purity of the perdeuterated myristic acid were determined by gas chromatography-mass spectrometry of the methyl ester to be 95–98%. Purity of the phospholipid was checked by thin layer chromatography, eluting with $CHCl_3$/MeOH/H_2O (65/35/5) followed by charring with 40% H_2SO_4, which yielded a single spot. Oriented lipid bilayer samples were prepared for ^2H NMR spectroscopy by first hydrating approximately 40 mg of the dry lipid in excess Tris buffer (about 70 wt. % buffer), containing 1 m*M* ethylenediaminetetraacetic acid (EDTA) at *p*H = 7.3. A small amount of this dispersion was placed on a 5 mm×14 mm glass cover slip (Corning No. 1). A second glass plate was then placed upon the first plate and was gently moved back and forth, shearing the lipid dispersion and slightly squeezing out the excess lipid. Next a portion of the lipid dispersion was placed on the dry top of the second glass plate, and covered with a third plate. The above procedure was repeated until about 20–30 glass plates separated by the hydrated lipid dispersion were stacked. The sample was dehydrated in a hydrating-rehydrating chamber above the main phase transition temperature T_m of the bilayer dispersion with a stream of heated nitrogen gas. After a single dehydration step, the sample was placed in a clean square glass tube (inner dimension 5 mm×5 mm) that served as the NMR sample chamber, and rehydrated in the presence of a cotton plug soaked with ^2H-depleted ^1H_2O (Aldrich, Milwaukee, WI). Successive hydration-dehydration cycles were carried out [84], and excess lipid was scraped from the edges and top of the stack before each rehydration step. The final hydrated sample was prepared for NMR spectroscopy by (i) placing square Teflon plugs on either side of the square glass tube, (ii) placing cotton balls soaked with ^2H-depleted ^1H_2O next to each of the Teflon plugs, and (iii) inserting a square silicone plug into each end of the square tube to seal the water inside.

NMR spectroscopy. Two spectrometers were utilized in the experiments reported herein, operating at magnetic field strengths of 7.06 and 11.7 T, respectively. An external amplifier (Henry Radio Tempo 2006-A, Los Angeles, CA) was used in series with the output of the radio frequency amplifier of each spectrometer to increase the output pulse magnitude. Each amplifier was capable of producing an adequately square pulse with a rise and fall time of about 500 ns. An external preamplifier (Miteq, Hauppauge, NY; model AU-2A-0150) was used for the experiments at 46.1 MHz, which had a 31 dB gain over the frequency range of 10–500 MHz, whereas at 76.8 MHz the preamplifier supplied with the instrument was employed. In order to keep high frequency noise from being introduced to the receiver, a low pass filter (Minicircuits, Brooklyn, NY; model BLP-70) was implemented in-line following the preamplifier. The quadrupolar echo pulse sequence, $(\pi/2)_\phi$-τ_1-$(\pi/2)_{\phi\pm 90}$-τ_2-acquire, was used to obtain the ^2H NMR spectra [85]. An eight-step phase cycle [86] was employed where the phase of the pulses is denoted by ϕ. Care was taken to calibrate the pulses and to obtain a very short $\pi/2$ pulse duration, with initiation of the

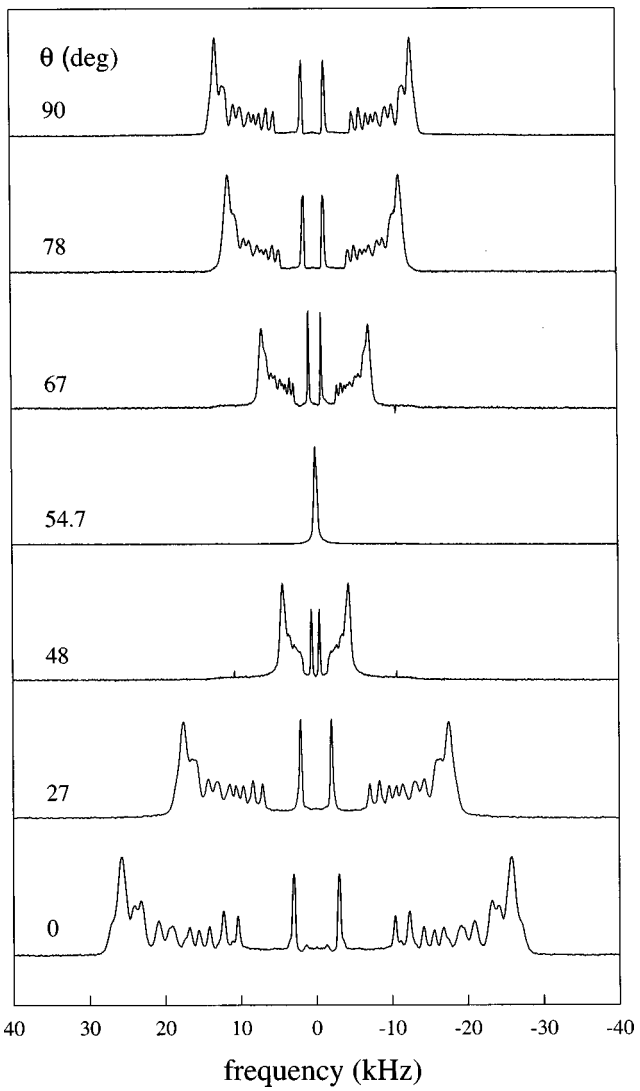

FIG. 2. Experimental ^2H NMR spectra measured at 46.1 MHz for macroscopically oriented DMPC-d_{54}, having perdeuterated acyl chains, in the L_α phase at $T = 40$ °C as a function of sample tilt angle θ ($\equiv \beta_{DL}$). As the sample tilt is increased from $\theta = 0°$, the spectrum contracts and finally collapses into a single line at the magic angle ($\theta = 54.7°$). This behavior is the result of axially symmetric effective motions of the phospholipids about the director axis of the lipid bilayer, i.e., the normal to the bilayer surface. Note that at the magic angle the quadrupolar splittings reverse sign, such that at the $\theta = 90°$ inclination they are scaled by a factor of $-1/2$ with respect to the $\theta = 0°$ tilt spectrum.

Fourier transformation at the top of the quadrupolar echo. Typical $\pi/2$ pulse widths were 1.8–2.3 μs for the experiments at 46.1 MHz, and 3.0–3.4 μs at 76.8 MHz, with delay times τ_1 and τ_2 of 30–40 μs. The quadrupolar splittings were fitted to the expression $\Delta\nu_Q = \frac{3}{2}\chi_Q S_{CD} d^{(2)}_{00}(\beta_{DL})$ for the whole tilt series, which enabled an accurate determination of a given sample inclination to within $\pm 1°$. The spin-lattice relaxation (R_{1Z}) rates were measured [14] using an inversion recovery pulse sequence, $(\pi)_\phi$-t_1-$(\pi/2)_\phi$-τ_1-$(\pi/2)_{\phi\pm 90}$-τ_2-acquire, by using a 32-step phase cycling routine [87]. Delay times t_1 ranged from 2 ms to 2 s depending on the T_{1Z} relaxation time of the sample. The time between successive experiments was at least three times the longest

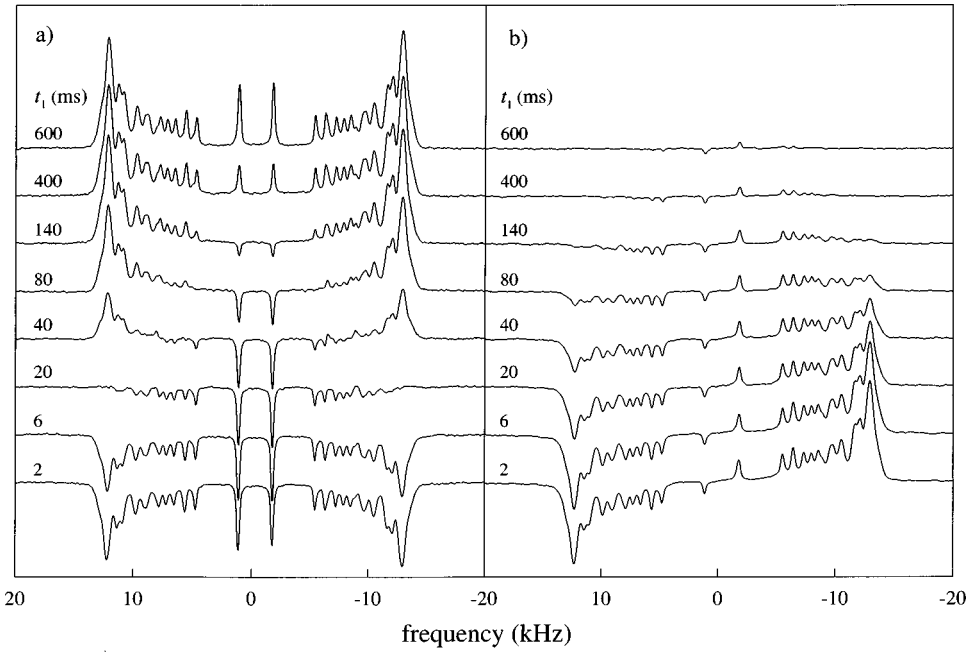

FIG. 3. Partially relaxed ^{2}H NMR spectra at 76.8 MHz showing the recovery of Zeeman order (R_{1Z}), part (a), and the decay of quadrupolar order (R_{1Q}), part (b), for bilayers of DMPC-d_{54} macroscopically oriented at $\theta = 90°$ in the L_α phase at $T = 40$ °C. The inversion recovery pulse sequence followed by the quadrupolar echo [14,85], was utilized for the ^{2}H R_{1Z} measurements; whereas the broadband Jeener-Broekaert sequence [51,88] was used for the ^{2}H R_{1Q} measurements. In parts (a) and (b) the partially relaxed ^{2}H NMR spectra are plotted at different delay times (t_1).

T_{1Z} in the sample. A three parameter fit was used to obtain the T_{1Z} values [75]. In order to measure the rate of the quadrupolar order decay (R_{1Q}) for oriented multilamellar dispersions of DMPC-d_{54}, a modified version of the Jeener-Broekaert pulse sequence was used [51]. The broadband Jeener-Broekaert pulse sequence developed by Wimperis [88] is ideally suited for ^{2}H NMR spectra with multiple quadrupolar splittings. A $\pi/2$ refocusing pulse was added to yield the sequence $(\pi/2)_\phi$-$2\tau_1$-$(3\pi/8)_{\phi-90}$-$2\tau_1$-$(\pi/4)_{\phi+90}$-τ_1-$(\pi/4)_{\phi+90}$-t_1-$(\pi/4)_\phi$-τ_2-$(\pi/2)_\phi$-τ_2-acquire, which was used to measure R_{1Q} relaxation rates. The first four pulses create quadrupolar order over a broad range of frequencies, and the subsequent pulses correspond to those previously described. Frequency dependent R_{1Z} measurements for small vesicles of DMPC deuterated at the C3 and C7 acyl chain segments have been previously described [27,44]; the data at 30 °C and 50 °C were interpolated by assuming an Arrhenius activation dependence to yield the values corresponding to 40 °C. To within experimental error there are few differences in the ^{2}H R_{1Z} relaxation rates of vesicles and multilamellar dispersions in this frequency range [14].

VI. RESULTS

A. General model-independent features of ^{2}H NMR relaxation in lipid bilayers

Representative experimental ^{2}H NMR spectra of macroscopically oriented bilayers of DMPC-d_{54} in the liquid-crystalline (L_α) state at different sample tilt angles ($\theta \equiv \beta_{DL}$) are shown in Fig. 2. The ^{2}H NMR spectra consist of multiple quadrupolar splittings, corresponding to the various segmental positions of the DMPC acyl chains, which decrease with the distance from the polar headgroup and reflect an increase in motional disorder along the chain [4]. As can be seen, increasing the tilt angle leads to a contraction of the spectrum, and at the magic angle of 54.7° all multiple quadrupolar splittings of the ^{2}H NMR spectrum collapse into one observed line. The assignments of the quadrupolar splittings to individual acyl chain segments as summarized by Dodd [83] are given in Table I. Note that the sharp doublet in the center of the spectrum corresponds to the methyl groups at the end of the DMPC acyl chains, which has an appreciably smaller splitting than the rest of the lines; this additional reduction of the residual quadrupolar coupling is the result of fast rotation about the methyl group axis.

The inversion recovery pulse sequence followed by the quadrupolar echo was used to measure the spin-lattice relaxation rates (R_{1Z}) at different sample tilt angles. Representative partially relaxed ^{2}H NMR spectra of macroscopically oriented DMPC-d_{54} in the L_α phase are shown in part (a) of Fig. 3. In addition, the broadband Jeener-Broekaert sequence [51,88,89] was to used to measure the quadrupolar order relaxation rates (R_{1Q}), which is illustrated in part (b) of Fig. 3. The experimental R_{1Z} and R_{1Q} relaxation rates at 46.1 and 76.8 MHz are summarized in Tables I and II, respectively. Figure 4 shows a typical dependence of the order parameter $S_{CD}^{(i)}$ (quadrupolar splitting), part (a), together with the $R_{1Z}^{(i)}$ and $R_{1Q}^{(i)}$ relaxation rates on the segment position or index i, parts (b) and (c), respectively. As can be seen from part (a) of Fig. 4, a plateau region corresponding to segments C3 through C6 is followed by a decrease of the order parameter due to increasing angular amplitudes of segmental motions along the acyl chains [4]. The analogous dependence takes place for the $R_{1Z}^{(i)}$ and $R_{1Q}^{(i)}$ relaxation rates, parts (b) and (c) of Fig. 4.

TABLE I. Spin-lattice (R_{1Z}) and quadrupolar order (R_{1Q}) relaxation rates for the sn-1 and sn-2 acyl chains of DMPC-d_{54} in the liquid-crystalline phase at 40 °C and 46.1 MHz.

Resonance	Acyl chain[a] segment			$R_{1Z}(\theta)$ (s^{-1})								$R_{1Q}(\theta)$ (s^{-1})				
	sn-1	sn-2	$\lvert S_{CD}\rvert$	$\theta=0°$	6.5°	20°	72°	78°	80°	86°	90°	0°	20°	80°	89°	90°
A	2-6	3-6	0.1926	32.4	33.8	33.9	36.9	37.6	38.2	37.4	39.0	34.8	32.4	29.8	30.6	29.7
				±1.6	±1.7	±1.7	±1.8	±1.8	±1.9	±1.8	±1.0	±1.9	±1.5	±1.5	±1.7	±1.6
B	7	7,8	0.1816	29.6	29.4	30.2	32.5	33.9	34.1	34.5	34.7	29.1	26.4	25.1	25.9	23.3
				±1.5	±1.5	±1.6	±1.7	±1.6	±1.7	±1.7	±1.9	±2.2	±2.0	±2.1	±2.0	±1.9
C	8	9	0.1696	25.6	26.2	26.3	31.3	33.9	33.5	33.2	32.8	27.7	25.2	23.0	22.8	22.6
				±1.2	±1.3	±1.2	±1.5	±1.6	±1.6	±1.6	±0.9	±1.4	±1.3	±1.4	±1.2	±1.3
D	9	10	0.1559	19.4	19.7	21.7	25.9	26.8	27.5	26.7	26.7	18.9	15.8	17.5	17.8	16.9
				±0.9	±1.0	±1.1	±1.4	±1.2	±1.2	±1.1	±1.2	±0.9	±1.1	±1.3	±1.2	±1.4
E	10	11	0.1455	16.6	18.0	18.0	23.3	23.9	23.4	22.9	23.1	16.9	17.6	14.3	14.2	13.8
				±0.9	±1.0	±0.9	±1.4	±1.4	±1.3	±1.1	±0.9	±1.7	±1.2	±1.4	±1.2	±1.2
F	11	2*b*	0.1291	14.7	15.5	18.5	21.0	20.9	21.2	20.6	20.4	15.4	18.2	16.1	13.2	11.5
				±0.7	±0.6	±0.9	±1.0	±0.8	±1.0	±0.9	±0.8	±1.2	±1.4	±1.1	±1.0	±0.9
G	12		0.1089	10.3	11.6	14.7	14.6	15.1	15.3	15.1	14.2	10.4	13.8	9.0	8.8	7.6
				±0.6	±0.7	±0.7	±0.8	±0.9	±0.8	±0.8	±0.6	±0.8	±1.0	±0.7	±0.9	±0.8
H	13		0.0897	8.6	10.3	9.9	10.8	10.6	10.2	9.9	9.6	8.8	7.6	6.5	5.8	4.8
				±0.7	±0.6	±0.8	±0.7	±0.8	±0.7	±0.8	±0.8	±0.9	±0.8	±0.6	±0.5	±0.5
I	14	14	0.0235	2.5	3.0	3.1	3.6	3.0	3.0	3.0	2.9	2.2	2.6	2.9	2.7	2.6
				±0.2	±0.2	±0.2	±0.1	±0.2	±0.3	±0.4	±0.2	±0.1	±0.1	±0.2	±0.2	±0.1

[a]Spectral assignments are from Ref. [83]. Only the data for the sn-1 acyl chain are fully summarized (9 out of a total of 11 resolved resonances).

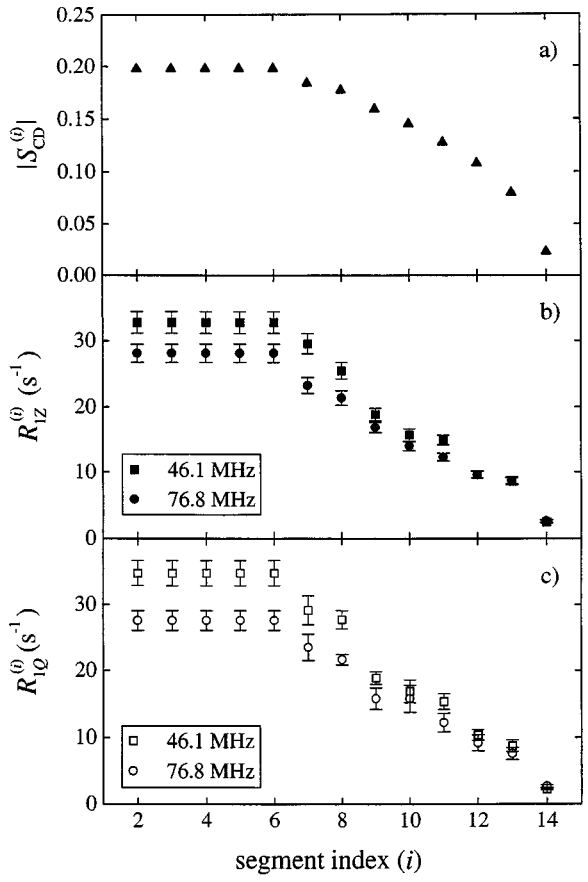

FIG. 4. Profiles of the segmental order parameters $S_{CD}^{(i)}$ (▲) measured at 76.8 MHz, part (a), and profiles of the ^{2}H $R_{1Z}^{(i)}$ and $R_{1Q}^{(i)}$ relaxation rates at 46.1 MHz (■, □, respectively) and 76.8 MHz (●, ○, respectively) as a function of acyl chain position (i), parts (b) and (c). The data are for the sn-1 acyl chain of DMPC-d_{54} macroscopically oriented at $\theta=0°$ in the L_α phase at $T=40$ °C. Both the order profile and the relaxation rate profiles are similar in shape and reveal a plateau region at the beginning of the chain, corresponding to segments C2–C6, followed by a progressive decrease thereafter.

Plots of the $R_{1Z}^{(i)}$ and $R_{1Q}^{(i)}$ relaxation rates as a function of the order parameter $S_{CD}^{(i)}$ squared at 76.8 MHz are presented in Fig. 5. One can see that the observed relaxation rates depend almost linearly on $|S_{CD}^{(i)}|^2$ along the entire acyl chain as proposed by Williams *et al.* [75]. An analogous square-law functional dependence of the $R_{1Z}^{(i)}$ and $R_{1Q}^{(i)}$ relaxation rates on the order parameter $S_{CD}^{(i)}$ is also observed at 46.1 MHz with a larger slope in all cases (results not shown) [45]. Such information can also be obtained from studies of phospholipids having specifically deuterated acyl chains [14,43], which are, however, substantially more time consuming in comparison with multilamellar dispersions of phospholipids having perdeuterated chains. As can also be seen from Fig. 5, the ordinate intercepts are less than 3 s^{-1}, which implies a rather small contribution from fast internal motions to the ^{2}H NMR relaxation rates of lipid bilayers in the MHz range.

Qualitatively, the angular dependent ^{2}H $R_{1Z}^{(i)}$ and $R_{1Q}^{(i)}$ relaxation rates of DMPC-d_{54} for the plateau region (Tables I and II) are similar to those obtained previously for bilayers of DMPC specifically deuterated at acyl positions C4 and C6 [20,28]. It is noteworthy that studies of phospholipids having perdeuterated acyl chains [33,34,51,75] are complementary to studies of phospholipids with specifically deuterated chains [12,14,20,28], in that the former enable one to investigate the behavior of the entire acyl chain as manifested in the angular anisotropy of the relaxation. For the case of DMPC-d_{54}, a qualitatively similar angular dependence of the ^{2}H R_{1Z} and R_{1Q} relaxation rates is obtained for the entire acyl chain (cf. Tables I and II), as also demonstrated in the case of DLPC-d_{46} [33]. The angular dependent $R_{1Z}^{(i)}$ and $R_{1Q}^{(i)}$ relaxation rates as a function of chain position appear to be simply scaled by the corresponding order parameter $S_{CD}^{(i)}$ squared, cf. Fig. 5, consistent within an interpretation in terms of order fluctuations (*vide supra*). Since frequency dependent relaxation data are available only for segments C3 and C7, the orientational anisotropies of DMPC-d_{54} have been analyzed in detail for these segments, i.e., for splittings A (plateau region) and B; cf. Tables I and II.

B. Fitting of experimental relaxation data to dynamical models

Simultaneous fits of model II (molecular diffusion), Eq. (3.4), to the experimental ^{2}H R_{1Z} and R_{1Q} relaxation rates for segments C3 and C7 of the DMPC acyl chains as a function of sample orientation and ^{2}H NMR frequency are presented in Fig. 6, and the fitting parameters are summarized in Table III. The R_{1Z} and R_{1Q} data at 46.1 MHz, parts (a) and (d), and at 76.8 MHz, parts (b) and (e), have been measured as a function of the sample orientation, and pertain to splittings A and B of oriented bilayers of DMPC-d_{54} in the L_α phase at 40 °C. The frequency dependent R_{1Z} relaxation rates are shown in parts (c) and (f) of Fig. 6 and correspond to previously published data for specifically deuterated DMPC vesicles at 30 °C and 50 °C [27,44], interpolated to 40 °C by assuming an Arrhenius activation dependence, which is obeyed within applicable accuracy for the ^{2}H NMR relaxation rates [14]. It should be noted that in the latter case the orientational averaging leads to $|D_{nm}^{(2)}(\Omega_{DL})|^2 \rightarrow \langle |D_{nm}^{(2)}(\Omega_{DL})|^2 \rangle = \frac{1}{5}$ and thus the projection index m vanishes in the spectral densities [43]. Both odd and even potentials of mean torque have been used for the molecular diffusion model [39,43,51]. The fact that the ^{2}H NMR spectrum collapses at the magic angle and that the observed relaxation rates depend on the square of the order parameter is in agreement with the occurrence of axially symmetric motions in the liquid-crystalline state of a lipid bilayer; therefore, one can set the effective asymmetry parameter η_Q^{eff} to zero; cf. Eq. (3.4). It has been further assumed that the average orientation of the z axis of the intermediate frame is nearly perpendicular to the long molecular axis [44], so that $\beta_{IM}=90°$. As can be seen, although the molecular diffusion model (II) describes the orientation dependence of the R_{1Z} and R_{1Q} relaxation rates rather well, it fails to describe the low-frequency dispersion of the orientationally averaged R_{1Z} data. Note that there is little difference between the results for the molecular diffusion with an even potential of mean torque and the model with an odd potential [33]. However, the value of $\lambda_1/kT=6.16$ in the latter case appears to be more plausible for the liquid-crystalline state; whereas the value of $\lambda_2/kT=2.91$ for an even potential of mean torque

TABLE II. Spin-lattice (R_{1Z}) and quadrupolar order (R_{1Q}) relaxation rates for the sn-1 and sn-2 acyl chains of DMPC-d_{54} in the liquid-crystalline phase at 40 °C and 76.8 MHz.

Resonance	Acyl chain[a] segment sn-1	sn-2	$\lvert S_{CD}\rvert$	$R_{1Z}(\theta)$ (s^{-1}) $\theta=0°$	12°	22°	27°	37°	39°	73°	81°	90°	$R_{1Q}(\theta)$ (s^{-1}) 0°	12°	22°	27°	40°	81°	89°	90°
A	2-6	3-6	0.2002	28.1	27.9	27.7	27.6	27.6	28.3	29.2	29.9	28.2	27.6	27.2	24.7	23.7	21.8	23.1	23.8	22.7
				±1.4	±1.4	±1.4	±1.4	±1.5	±1.4	±1.7	±1.5	±1.4	±1.5	±1.6	±1.3	±1.5	±1.5	±1.2	±1.1	±1.2
B	7	7,8	0.1859	23.2	23.0	23.0	22.5	25.4	25.4	27.0	27.5	25.5	23.5	23.6	20.8	21.1	18.6	18.6	20.6	18.5
				±1.2	±1.2	±1.2	±1.1	±1.3	±1.3	±1.4	±1.6	±1.4	±2.0	±1.5	±1.1	±1.1	±0.9	±1.0	±0.9	±0.9
C	8	9	0.1793	21.4	21.7	22.7	22.5	25.4	25.5	27.2	27.5	25.5	21.6	22.2	18.6	20.2	17.7	18.6	20.2	18.5
				±1.1	±1.1	±1.2	±1.2	±1.2	±1.2	±1.5	±1.1	±1.2	±0.8	±1.8	±1.1	±1.1	±0.6	±0.9	±0.9	±0.7
D	9	10	0.1612	16.9	16.6	16.8	17.1	19.0	19.3	21.2	22.1	20.6	15.8	16.6	18.6	16.2	15.5	14.0	15.2	14.0
				±0.8	±0.8	±0.9	±0.9	±1.3	±1.0	±1.1	±1.1	±1.1	±1.6	±0.6	±0.8	±0.8	±1.3	±0.7	±0.7	±0.7
E	10	11	0.1471	14.0	14.6	14.6	16.2	17.2	17.7	18.7	19.9	17.8	15.7	14.6	14.4	14.9	13.7	11.0	12.6	11.4
				±0.7	±0.8	±0.7	±0.8	±1.0	±0.8	±0.9	±0.9	±1.1	±2.0	±1.2	±0.8	±1.4	±1.7	±0.5	±0.6	±0.4
F	11	2*b*	0.1292	12.3	12.4	14.5	16.4	14.4	16.6	17.1	17.4	15.7	12.2	13.7	14.0	15.3	11.7	10.2	12.3	10.9
				±0.6	±0.6	±0.7	±0.8	±0.9	±0.9	±0.9	±0.9	±0.8	±1.4	±0.6	±0.6	±1.2	±1.2	±0.5	±0.4	±0.5
G	12		0.1093	9.6	10.9	11.5	10.6	11.2	11.8	12.4	13.0	11.7	9.1	11.5	11.6	9.9	8.7	7.7	8.1	6.5
				±0.5	±0.5	±0.6	±0.6	±0.8	±0.6	±0.7	±0.7	±0.7	±1.2	±0.7	±0.6	±0.4	±0.4	±0.4	±0.5	±0.4
H	13		0.0803	8.6	8.2	8.1	7.7	8.1	8.4	8.7	8.7	8.2	7.6	8.4	8.3	6.8	6.4	4.7	6.0	5.3
				±0.5	±0.6	±0.6	±0.5	±0.6	±0.6	±0.6	±0.7	±0.8	±0.9	±0.8	±0.5	±0.8	±0.5	±0.4	±0.4	±0.3
I	14	14	0.0232	2.6	2.7	2.6	2.6	2.6	2.8	3.0	2.9	2.8	2.7	2.2	3.1	3.4	2.8	2.1	2.5	2.9
				±0.2	±0.1	±0.2	±0.1	±0.2	±0.1	±0.2	±0.3	±0.1	±0.2	±0.4	±0.3	±0.1	±0.5	±0.3	±0.3	±0.2

[a]Spectral assignments are from Ref. [83]. Only the data for the sn-1 acyl chain are fully summarized (9 out of a total of 11 resolved resonances).

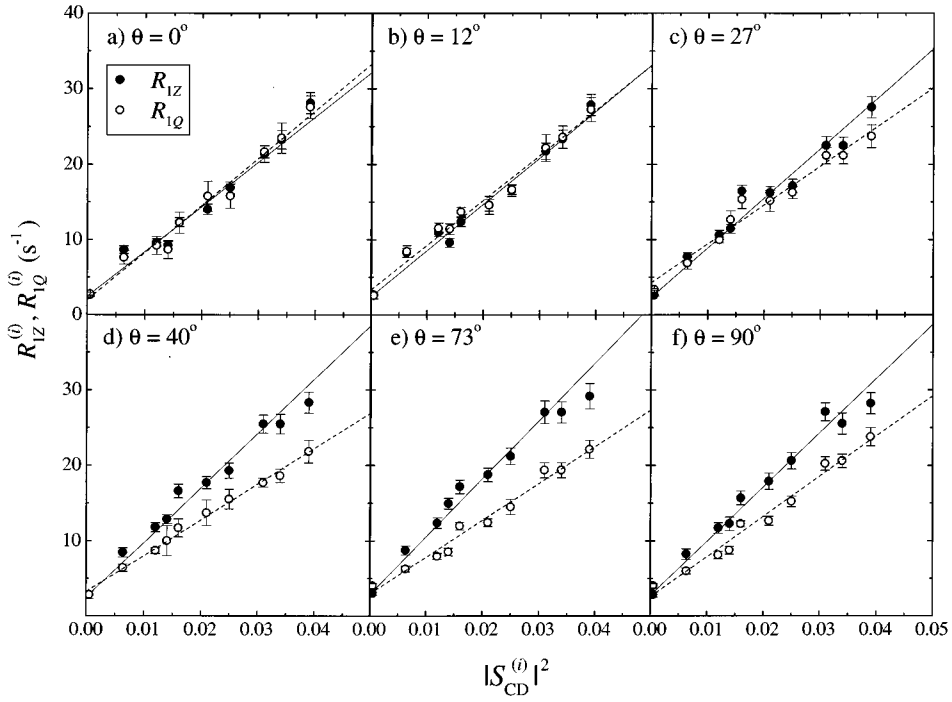

FIG. 5. ^{2}H NMR relaxation rates $R_{1Z}^{(i)}$ (●) and $R_{1Q}^{(i)}$ (○) at 76.8 MHz for DMPC-d_{54} in the L_α phase at $T=40$ °C plotted as a function of the square of the experimentally observed order parameter $|S_{CD}^{(i)}|$. Sample tilt angles: part (a), $\theta=0°$; part (b), 12°; part (c), 27°; part (d), 40°; part (e), 73°; and part (f), 90°. A linear dependence of both the $R_{1Z}^{(i)}$ and $R_{1Q}^{(i)}$ relaxation rates on the order parameter squared is observed along the entire acyl chain. This square-law functional dependence appears to be a characteristic feature of the spin relaxation in saturated lipid bilayers, and manifests preaveraging of the static coupling tensor by faster motions.

TABLE III. Summary of fitting parameters. All simultaneous curve fitting has been done by using the Levenberg-Marquardt algorithm. The fits have been statistically weighted by the inverse square of the standard deviation [94].

Model	$D_\parallel(10^9$ s$^{-1})$	$D_\perp(10^7$ s$^{-1})$	λ_j or λ/kT[a]	$S_s^{(2)}$	$\tau_c(10^{-7}$ s)	$D(10^{-5}$ s$^{1/2})$	$\omega_c(10^{10}$ s$^{-1})$	R_{int}(s^{-1})	χ_v^2
Molecular diffusion (model II, even potential)	3.53±0.36	8.14±0.67	2.91±0.07	0.593				0	8.04
Including slow motions	3.29±0.41	10.1±0.2	2.96±0.14	0.600	1.57±0.22			0[b]	9.91
Molecular diffusion (model II, odd potential)	3.49±0.40	9.87±1.00	6.16±0.23	0.592				0	9.68
Including slow motions	3.72±0.31	11.8±0.1	5.91±0.17	0.578	1.78±0.19			0.00[c]	4.49
3D director fluctuations (model IV; linear order)						3.91±0.13	∞	0[b]	20.1
Linear+quadratic orders			0.178±0.029	0.466			1.74±2.17	0[b]	30.4
Composite model (model V; even potential)	1.73±0.10	0.419±0.135	8.89±1.19	0.882		1.08±0.08	∞	0[b]	4.55
Including R_{int}	4.47±1.42	0.717±0.168	6.97±0.81	0.847		0.678±0.127	∞	12.2±2.5	3.36
Composite model (model V; odd potential)	1.82±0.12	0.523±0.171	21.9±3.4	0.869		1.02±0.09	∞	0[b]	4.41
Including R_{int}	4.50±1.47	0.728±0.178	18.4±2.59	0.845		0.681±0.130	∞	12.3±2.6	3.37

[a]The energy parameter λ_j is for the case of the molecular diffusion model (II) whereas λ is for collective fluctuations (IV), Eq. (3.8).
[b]Parameter held constant at this value.
[c]Parameter value at which $D_\parallel$ can be determined with applicable accuracy.

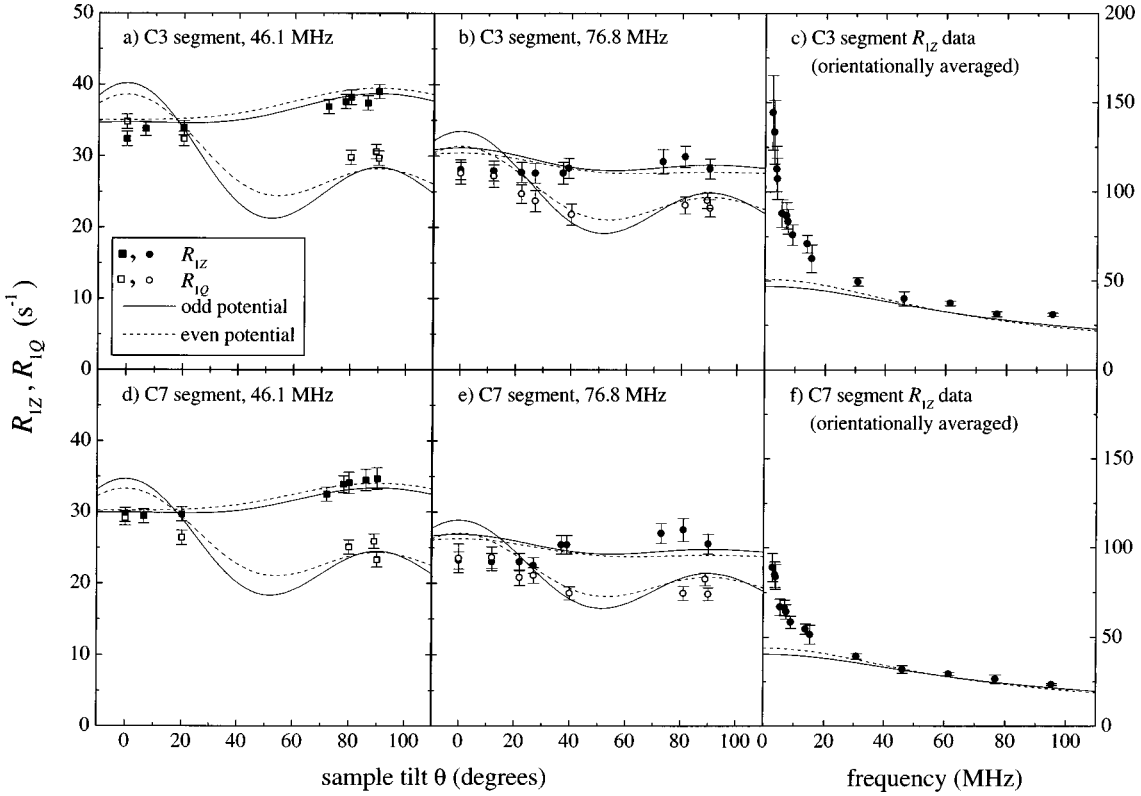

FIG. 6. Simultaneous theoretical fitting of ^{2}H R_{1Z} (■, ●) and R_{1Q} (□, ○) relaxation rates as a function of bilayer orientation and frequency to the noncollective molecular diffusion model (II). Results are shown for acyl chain segments C3 and C7 of DMPC-d_{54}, i.e., splittings A and B, in the L_α phase at $T=40$ °C as a function of bilayer orientation at 46.1 MHz, parts (a) and (d), and 76.8 MHz, parts (b) and (e), together with orientationally averaged ^{2}H R_{1Z} data for DMPC vesicles as a function of frequency (magnetic field strength), parts (c) and (f). Both an odd potential (—) and an even potential (– – – –) of mean torque have been used; cf. the text. The data are summarized in Tables I and II and the fitting parameters are presented in Table III. The model describes the behavior of the relaxation rates as a function of sample orientation, although marked deviations are found in the case of the frequency dispersion, especially at low frequencies. Note that there is little difference in the quality of the fits between the odd potential of mean torque and the even potential.

(Table III) would correspond to a lower energy barrier and, therefore, to a more unstable membrane at 40 °C. In Fig. 7 we have attempted to further improve the quality of the fits of model II to the R_{1Z} relaxation rates of DMPC vesicles by including a Lorentzian spectral density corresponding to additional slow motions, e.g., vesicle tumbling [39], in the overall spectral densities of motion, Eq. (3.4). However, even in this case marked deviations in the frequency dependence are found; cf. Fig. 7. Note that the molecular diffusion with an odd potential of mean torque better corresponds to the data than in the case of an even potential.

The fits to the membrane deformation model (3D director fluctuations; model IV), which takes into account linear-order director fluctuations, Eq. (3.7), is illustrated in Fig. 8, and the fitting parameters are included in Table III. Despite the fact that the model fits the frequency dependent R_{1Z} data for DMPC vesicles in terms of an $\omega^{-1/2}$ relaxation law [16,27,37], it fails to describe simultaneously the orientationally dependent R_{1Z} and R_{1Q} data for the oriented DMPC-d_{54} samples. To ascertain whether this may be a result of neglecting higher-order terms of director fluctuations, the more detailed expression [70] that also takes into account quadratic terms, Eq. (3.8), has been used. As can be seen in Fig. 8, even in this case, the model does not simultaneously fit the orientation dependence of the R_{1Z} and R_{1Q} relaxation rates. This may imply that model IV alone is not suitable for the description of the ^{2}H NMR relaxation in lipid bilayers.

Therefore, the next step was to combine models II and IV, noting their complementary abilities to fit separately the orientation and frequency dependence, respectively. The fits of the data to the composite model (V), which takes into account both the noncollective and collective motions, Eq. (4.6), are shown in Fig. 9, and the fitting parameters are presented in Table III. Clearly, an improvement of the quality of the fits is observed versus the previous models which describe only one type of motion. Both odd and even potentials of mean torque were used, which yielded little or no difference in the quality of the fits as in the case of model II alone. Comparison of the fitting parameters obtained for the composite membrane deformation model (V) with those for the fit to the molecular diffusion model (II) only, shows a decrease in the diffusion coefficient $D_\perp$ and larger values for λ_j/kT, cf. Table III. Using Eq. (3.6), one obtains for the slow molecular order parameter a value of $S_s^{(2)}=\langle D_{00}^{(2)}(\Omega_{MN})\rangle=0.9$ in the case of the composite model (V) versus $S_s^{(2)}=\langle D_{00}^{(2)}(\Omega_{MD})\rangle=0.6$ for the molecular diffusion model (II), which yields a decreased molecular ordering. It should be also noted that the fitting parameters describing the noncollective molecular rotations in the presence of collective fluctuations are close to those obtained previously from fitting the noncollective molecular diffusion model to the

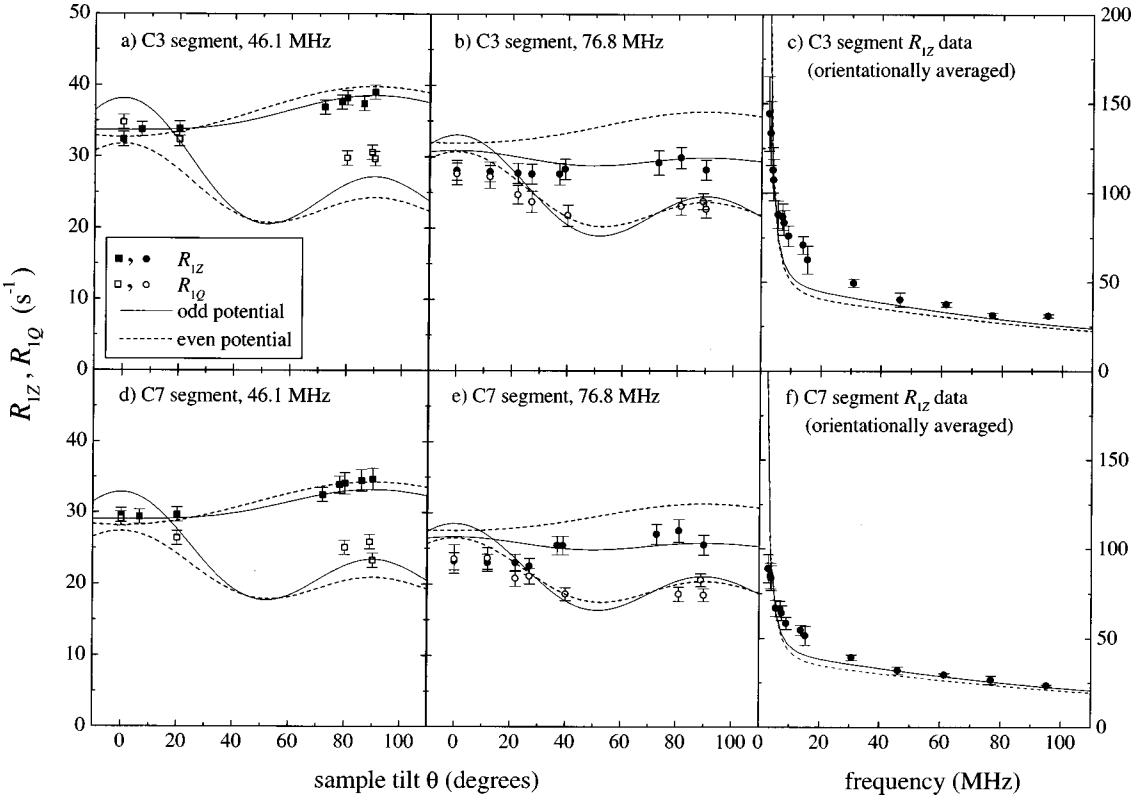

FIG. 7. Simultaneous theoretical fitting of ^{2}H R_{1Z} (■, ●) and R_{1Q} (□, ○) relaxation rates as a function of bilayer orientation and frequency to the noncollective molecular diffusion model (II) including an additional slow motion term. Data are included for acyl chain segments C3 and C7 of DMPC-d_{54}, i.e., splittings A and B, in the L_α phase at $T=40$ °C as a function of bilayer orientation at 46.1 MHz, parts (a) and (d), and 76.8 MHz, parts (b) and (e), as well as orientationally averaged ^{2}H R_{1Z} data for DMPC vesicles as a function of frequency (magnetic field strength), parts (c) and (f). An odd potential (—) and an even potential (– – – –) of mean torque have both been used; cf. the text. The data are included in Tables I and II and the fitting parameters are summarized in Table III. Even though the noncollective model describes the behavior of the relaxation rates as a function of sample orientation and frequency, the quality of the fits is not very good. Note that the model with an odd potential of mean torque better corresponds to the data than the model with an even potential.

frequency dispersion only [44]. Including an empirical contribution from internal fast motions further improves the quality of the fits, as expected due to an increase in the number of fitting parameters, but yields a relatively large value of $R_{\rm int}=12\ {\rm s}^{-1}$, which is not completely consistent with the above conclusion about a small contribution from internal motions [16,43]. If only the noncollective molecular diffusion model is used to fit the data, an even greater value of $R_{\rm int}=21\ {\rm s}^{-1}$ is obtained [39], which also increases the uncertainty in determining the axial diffusion coefficient, $D_\parallel$. Therefore, at present it seems more consistent to disregard the empirical term $R_{\rm int}$ in the modeling, and consider instead just the preaveraged amplitudes due to the fast segmental motions that result in the observed order parameter in the ^{2}H NMR spectra.

The behavior of the ^{2}H R_{1Z} and R_{1Q} relaxation rates obtained at two frequencies of 46.1 and 76.8 MHz for the entire acyl chain of DMPC-d_{54} is shown in Fig. 10. As can be seen from the simulations, both the composite membrane deformation model and the molecular diffusion model describe comparably the experimental data along the entire acyl chain with the fitting parameters summarized in Table III, except for segments toward the end of the acyl chain, splittings G-I. The systematic underestimation of the experimental relaxation rates may indicate the presence of a contribution from fast internal motions $R_{\rm int}$ of about 3 s^{-1}, which is consistent with the intercept values obtained from the linear square-law dependence of the relaxation rates on the order parameter $S_{\rm CD}$, as shown in Fig. 5. A drawback of studying chain-perdeuterated lipids is that although the entire chain can be investigated, overlap of the splittings precludes detailed investigation if the sample tilt is set near the magic angle (54.7°). It should be noted, however, that both models predict a dip near the magic angle in the ^{2}H R_{1Q} orientational anisotropy, in agreement with the relaxation data measured for specifically deuterated lipids [20], cf. Fig. 1. To further test the above models describing slow order fluctuations, the orientationally dependent data for another representative lipid system, POPC-d_{31} [34], have been fitted simultaneously for segments C5, C8, C10, and C13 of the palmitoyl acyl chain (results not shown). Both the molecular diffusion model (II) and the composite membrane deformation model (V) describe the data satisfactorily; whereas the 3D director fluctuation model (IV) does not account for the orientational anisotropy of POPC-d_{31}, as also found in the case of DMPC-d_{54}. However, since the data for POPC-d_{31} were measured at only one frequency (46.2 MHz) [34], no defini-

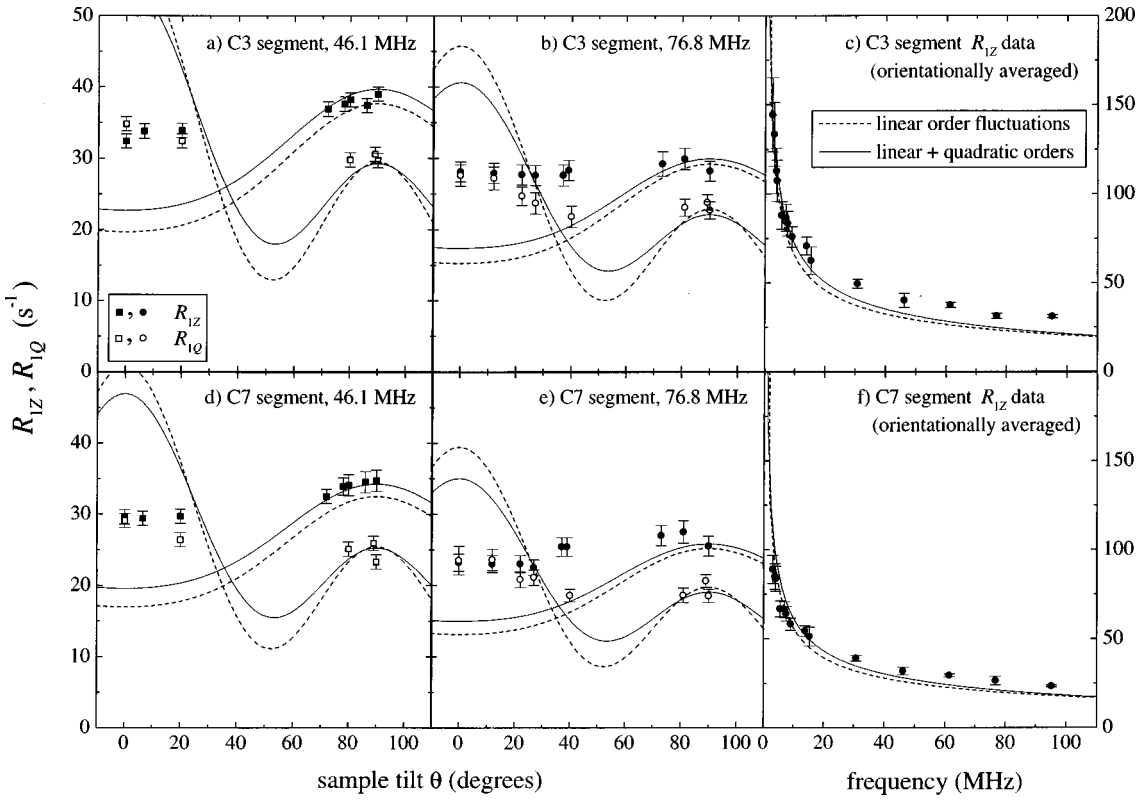

FIG. 8. Simultaneous theoretical fitting of ^{2}H R_{1Z} (■, ●) and R_{1Q} (□, ○) relaxation rates as a function of bilayer orientation and frequency to the membrane deformation model (3D collective fluctuations; model IV). Results are shown for acyl chain segments C3 and C7 of DMPC-d_{54}, i.e., splittings A and B, in the L_α phase at $T=40\,^\circ$C as a function of bilayer orientation at 46.1 MHz, parts (a) and (d), and 76.8 MHz, parts (b) and (e), as well as orientationally averaged ^{2}H R_{1Z} data for DMPC vesicles as a function of frequency (magnetic field strength), parts (c) and (f). The data are fitted for the case of linear-order director amplitudes (– – – –) [44] and for the case of linear + quadratic orders (—) [70], cf. the text. Tables I and II present the data and the fitting parameters are given in Table III. The model accounts for the frequency dispersion, but fails to describe simultaneously the orientation dependent relaxation data in both cases. The deviation of the model from experiment is significant, which may mean that the 3D collective model alone is not suitable for a description of the ^{2}H NMR relaxation rates in lipid bilayers.

tive conclusion about the collective part of the composite model can be made, since the corresponding parameter D characterizing the collective motions cannot be determined to sufficient accuracy.

For the composite membrane deformation model (V), the individual contributions from noncollective and collective motions as well as the contribution of the cross-term, Eq. (4.7), to the ^{2}H R_{1Z} relaxation rates of DMPC in the L_α state are shown in Fig. 11. The data refer to the initial part of the DMPC acyl chains, C2–C6 and C3 segments in parts (a) and (b), respectively. Within the mid-MHz range these contributions are of the same order for both the orientation dependence at 76.8 MHz, part (a), as well as at 46.1 MHz (results not shown), and for the frequency dispersion, part (b). At lower frequencies, however, the time-scale separation between the noncollective and collective motions becomes more pronounced, and the collective motions become predominant; as a result, the cross-term has a much smaller relative contribution, cf. part (b) of Fig. 11. Figure 12 shows the director-frame spectral densities of motion $J_p^{\rm dir}(\omega)$ for segments C2–C6 (plateau region), calculated at four frequencies by using Eqs. (2.4), (2.8), and (2.9) for the composite model (V), Eq. (4.6). Note that the combination of Eqs. (2.4), (2.8), and (2.9) represents in fact an overdetermined system of linear equations, each corresponding to measurement of the relaxation rates at a given sample tilt angle $\beta_{DL}\equiv\theta$ and Larmor frequency ω. Therefore, the six director-frame spectral densities $J_p^{\rm dir}(\omega)$, where $p=0$, 1, 2, and $\omega=\omega_{\rm D},2\omega_{\rm D}$, can be regarded as independent variables or fitting parameters, and can be obtained from a linear regression fit without invoking a particular model. As can be seen from Fig. 12, the spectral density $J_1^{\rm dir}(\omega)$ is larger than $J_0^{\rm dir}(\omega)$ and $J_2^{\rm dir}(\omega)$ as also predicted by the composite model (V). Note that only the spectral density $J_1^{\rm dir}(\omega)$ contains the contribution from the collective motions in the small-amplitude approximation for director fluctuations, cf. Eqs. (3.7) and (4.6); this may explain the fact that $J_1^{\rm dir}(\omega)$ has the largest value, cf. also Nagle [90]. The same trend is observed for the rest of the segments of the DMPC-d_{54} acyl chains (not shown), but the error in determining the spectral densities rises significantly with the segment number. The rather poor correspondence of the theory to the calculated values of the spectral densities may be a consequence of propagation of errors from the experimental relaxation rates when calculating the laboratory-frame spectral densities by using Eqs. (2.8) and (2.9), together with the fitting procedure involved in calcu-

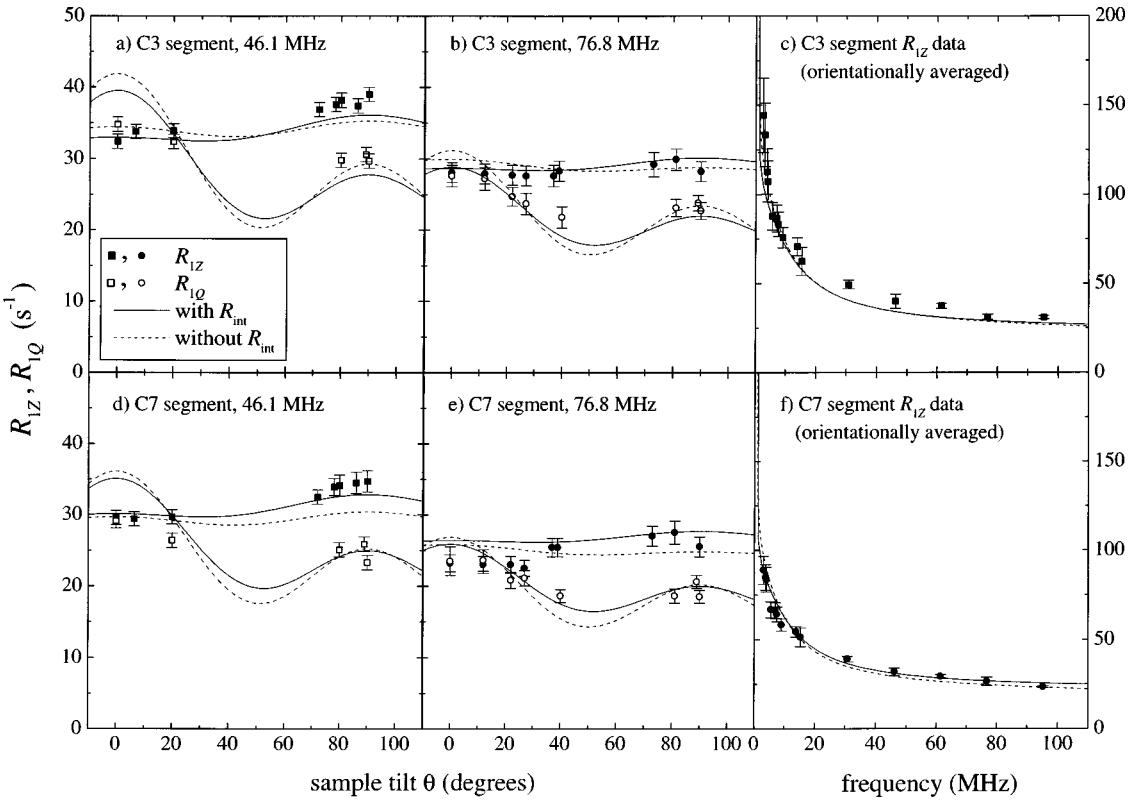

FIG. 9. Simultaneous theoretical fitting of ^{2}H R_{1Z} (■, ●) and R_{1Q} (□, ○) relaxation rates as a function of bilayer orientation and frequency to the composite membrane deformation model (V), taking into account the effect of molecular diffusion in the presence of an odd potential of mean torque and 3D director fluctuations (−−−−). Data are included for acyl chain segments C3 and C7 of DMPC-d_{54}, i.e., splittings A and B, in the L_α phase at $T=40$ °C as a function of bilayer orientation at 46.1 MHz, parts (a) and (d), and 76.8 MHz, parts (b) and (e), together with orientationally averaged ^{2}H R_{1Z} data for DMPC vesicles as a function of frequency (magnetic field strength), parts (c) and (f). No additional slow-motional term was needed to fit simultaneously the R_{1Z} and R_{1Q} relaxation rates. The data are presented in Tables I and II and the fitting parameters are included in Table III. Compared to the noncollective molecular diffusion model (II) and the 3D director fluctuation model (IV) alone, a significant improvement of the quality of the fits is achieved, which suggests that both types of motions may influence the ^{2}H NMR relaxation within the mid-MHz scale. Inclusion of a contribution from internal fast motions (—) further improves the quality of the fits, but yields a relatively large value of $R_{int}=12.3\ s^{-1}$.

lating the director-frame spectral densities, Eq. (2.4). Therefore, despite its apparent model-free features, the direct calculation of the director-frame spectral densities for the macroscopically oriented samples turns out to be very sensitive to the experimental error of the relaxation rate measurements.

VII. DISCUSSION

In this research an extensive body of ^{2}H R_{1Z} and R_{1Q} relaxation data for DMPC in the liquid-crystalline state has been analyzed simultaneously, which has yielded valuable information about the relative contributions of different types of motions to the nuclear spin relaxation in lipid bilayers. An important observation is that in the case of pure lipid bilayers the ^{2}H R_{1Z} and R_{1Q} relaxation rates are scaled by the corresponding order parameter squared (quadrupolar splitting), which holds for the entire acyl chain of DMPC-d_{54} at all sample orientations. This is interpreted as an effect of preaveraging of the effective coupling tensor left over from fast local motions, which points at a complex hierarchy of motions affecting the ^{2}H NMR relaxation of lipid bilayers within the MHz range. The simplest ''model-free'' strong-collisional formulation is most probably not suitable for a description of the lipid dynamics, and more detailed models taking into account the molecular geometry and local fast motions must be analyzed. Previous results have shown that a segmental diffusion model (I), which was found to fit the orientationally dependent data [33], does not adequately account for the frequency dispersion of the relaxation rates [44]. Another approach, somewhat different from the treatment of continuous diffusive reorientations, is to consider the segmental or molecular motions as multiple-site jumps [52], which has been successful in describing the angular anisotropy of nuclear spin relaxation rates [18,22,23] in lipid bilayers. However, jump models do not yield the square-law functional dependence on the order parameter [43,75], which is experimentally observed over a broad range of sample tilt angles in the MHz frequency range [33]. In addition, the jump correlation times predicted by these models fall into the subnanosecond scale [23], which again would lead to little or no frequency dispersion within the frequency range considered in the present paper. By contrast, a dramatic frequency dependence of the experimental relaxation rates, especially

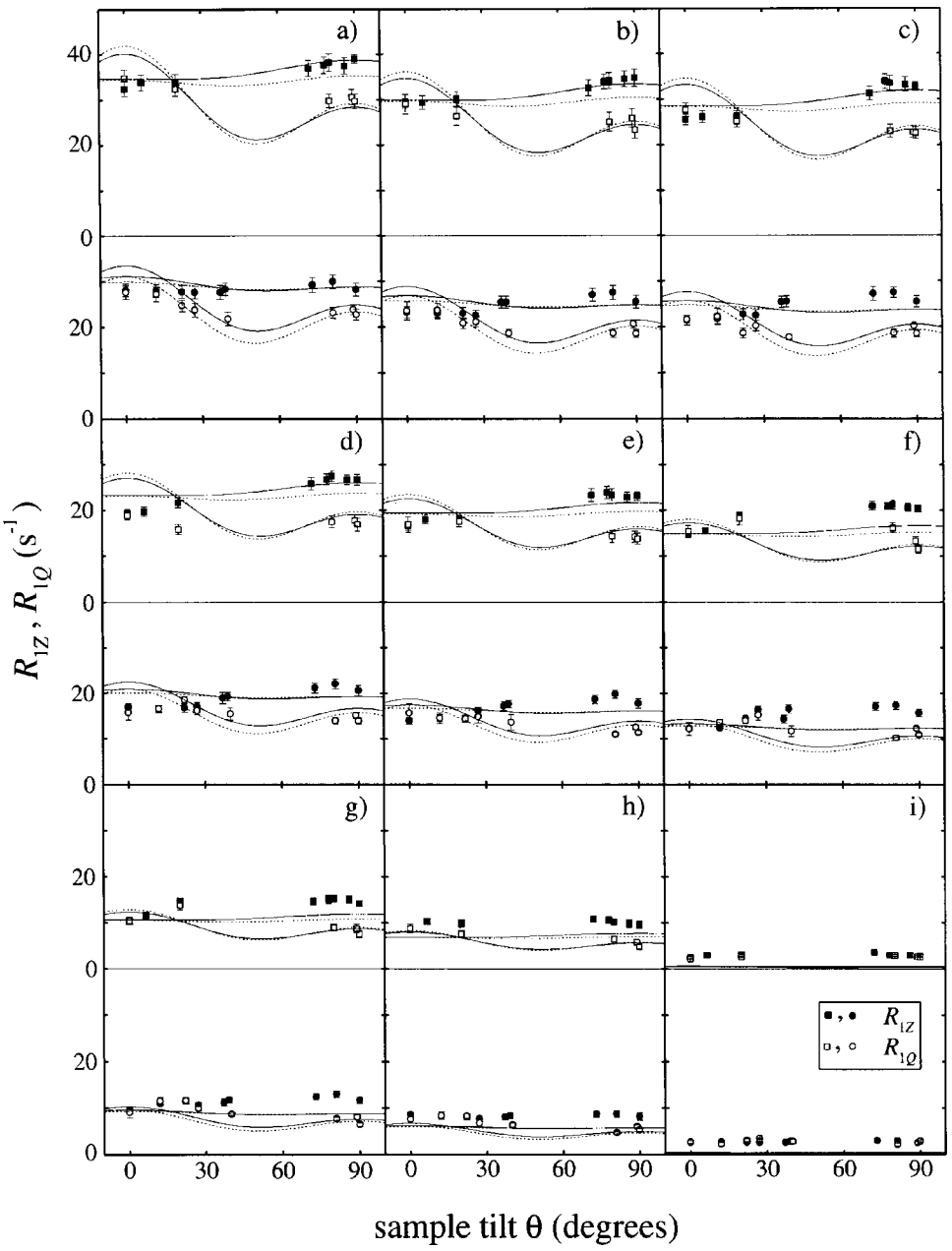

FIG. 10. Simulation of ^{2}H R_{1Z} and R_{1Q} relaxation rates for the entire acyl chain of DMPC-d_{54} as a function of bilayer orientation at two different frequencies (46.1 and 76.8 MHz). The experimental data are summarized in Tables I and II and the fitting parameters are presented in Table III. Parts (a)–(i) include ^{2}H R_{1Z} relaxation rates at 46.1 MHz (■) and 76.8 MHz (●), and R_{1Q} relaxation rates at 46.1 MHz (□) and 76.8 MHz (○) for the resolved quadrupolar splittings (designated $A-I$) of DMPC-d_{54} in the L_α phase at $T=40\,°C$. The composite membrane deformation model including both molecular and collective motions (– – – –) as well as the limiting case of molecular motions only (—) has been considered. In both cases satisfactory fits are obtained except for segments close to the end of the acyl chain, resonances $G-I$, which is due to neglect of the contribution from fast internal motions R_{int}.

in the low-MHz range, is observed in the case of vesicles and multilamellar dispersions [16,27].

Here various dynamical models describing order fluctuations, due to relatively slow noncollective molecular motions as well as collective bilayer excitations, have been fitted to the orientation dependent ^{2}H R_{1Z} and R_{1Q} relaxation rates for macroscopically oriented DMPC-d_{54} bilayers, together with the frequency dispersion for vesicles of ^{2}H-labeled DMPC at 40 °C. The combined analysis of the relaxation rates as a function of more than one variable provides a more rigorous basis for testing and eliminating some dynamical models, and for accepting others. For example, a simple molecular diffusion model (II) accounts for the relaxation orientational anisotropy [33,71], but is less satisfactory in explaining the frequency dispersion of the ^{2}H R_{1Z} relaxation rates [27,44]. The above would leave the noncollective molecular diffusion model (II) including an additional slow-motion term [39] as a potential candidate for the description of nuclear spin relaxation in lipids. However, the quality of the fits of the model to the frequency dispersion is still not

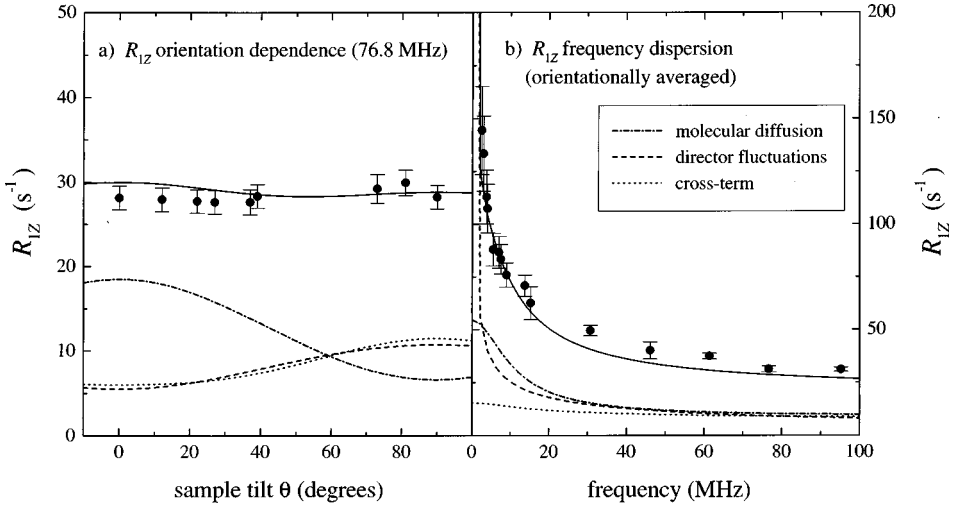

FIG. 11. Contributions of different types of motions to ^{2}H R_{1Z} relaxation rates (●) for the initial part of the acyl chains of DMPC in the liquid-crystalline state at $T=40$ °C. Theoretical R_{1Z} values without $R_{\rm int}$ (—); molecular diffusion contribution (–·–·–·–); director fluctuation contribution (––––); and cross-term (·····). (a) Motional contributions at 76.8 MHz as a function of bilayer orientation (θ) for multilamellar dispersions of DMPC-d_{54}, C2–C6 segments. (b) Motional contributions to the orientationally averaged frequency dependent R_{1Z} relaxation rates for vesicles of DMPC ^{2}H-labeled at C3 acyl segment. At higher frequencies the contributions from molecular diffusion in the presence of an odd potential (–·–·–·–) and 3D director fluctuations (––––) are of the same order. By contrast, at lower frequencies the time-scale separation between the noncollective and collective motions is greater. As a result, the collective motions become predominant and the cross-term (·····) has a smaller relative contribution.

completely satisfactory. On the other hand, the membrane deformation model (3D collective fluctuations; model IV), which accounts for the frequency dispersion of DMPC vesicles [27,37,44], fails to describe the orientation dependence of the ^{2}H R_{1Z} relaxation rates [20] (this work). One might argue that the fact that the 3D director fluctuation model (IV) does not fit the orientation dependent relaxation data may be connected with the assumption about the linear order of director fluctuation amplitudes, leading to vanishing of the collective director spectral densities $J_0^{\rm dir}(\omega)$ and $J_2^{\rm dir}(\omega)$. However, consideration of higher-order fluctuations, e.g., correlation functions of the order $\langle \beta_{ND}(t+\tau)^2 \beta_{ND}(t)^2 \rangle$ [70], only slightly changes the fits, and an obviously greater modification of model IV is needed since the theoretical orientation dependence of the ^{2}H R_{1Z} and R_{1Q} relaxation rates, as predicted by the model, does not correspond to the experimental data.

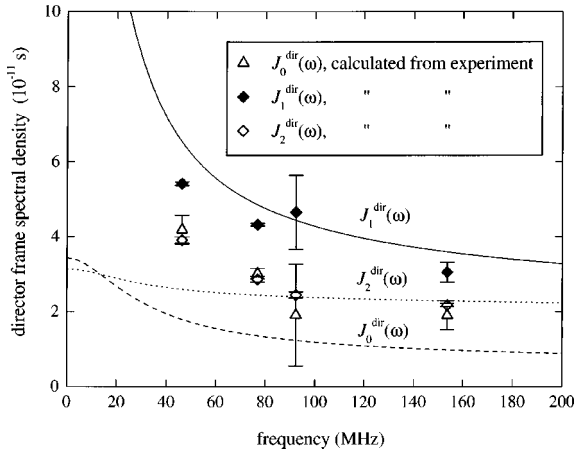

FIG. 12. Director-frame spectral densities of motion calculated from ^{2}H R_{1Z} and R_{1Q} relaxation rates for C2–C6 acyl segments of DMPC-d_{54} in the L_α phase at $T=40$ °C. Spectral density $J_0^{\rm dir}(\omega)$, experiment (△) and theory (––––); spectral density $J_1^{\rm dir}(\omega)$, experiment (◆) and theory (—); and spectral density $J_2^{\rm dir}(\omega)$, experiment (◇) and theory (·····). For the entire DMPC-d_{54} acyl chain the experimental spectral densities follow the trend $J_1^{\rm dir}(\omega) > J_0^{\rm dir}(\omega) \approx J_2^{\rm dir}(\omega)$. Note that only the $J_1^{\rm dir}(\omega)$ term contains the effect of the collective fluctuations to linear order in the director amplitudes. The relatively large errors of the experimental values are most probably a consequence of the propagation of errors involved in calculating the director-frame spectral densities, cf. the text. The general trends of the theoretical spectral densities and the values calculated directly from the experimental data are in agreement with each other.

Consequently, we propose herein a composite membrane deformation model for lipid bilayers that includes small-amplitude director fluctuations in the presence of molecular rotations. The improvement of the fits, especially in the case of the frequency dispersion of DMPC vesicles, implies that small-amplitude director fluctuations substantially influence the ^{2}H NMR relaxation [43] together with molecular diffusion [21,39,43], and can be detected in the mid-MHz frequency scale. The three-dimensional character of the collective fluctuations suggests the presence of uncoupled undulatory excitations, which would correspond to a nematiclike picture for the bilayer interior, with wavelengths of excitations ranging from the segmental dimensions up to the bilayer thickness. At longer distances and lower frequencies, a transition to two-dimensional director fluctuations described by a flexible surface model [44,64,65] is expected, as theoretically analyzed recently by Halle and Gustafsson [78].

An important feature of the membrane deformation model is the treatment of the cutoff for the wave vector q_c, which is set to infinity yielding a simple $\omega^{-1/2}$ frequency dependence. The justification for this assumption is based on the

fact that, if one considers a finite value for q_c, then a relatively high value for the cutoff frequency $\omega_c \equiv Kq_c^2/\eta = 1.74\times10^{10}$ rad s^{-1} is obtained, which allows one to set $u(\omega/\omega_c)\approx 1$ corresponding to an effectively infinite frequency cutoff. At the same time, however, the value of the slow order parameter [70] $S_s^{(2)} = 1-3\lambda/kT$ remains finite, where $\lambda/kT \equiv kTq_c/2\pi^2K$. Assuming the value for q_c to be roughly on the order of the inverse of the segmental dimensions, i.e., ≈ 1 Å^{-1}, one can estimate the bilayer elasticity K and the viscosity coefficient η for bilayer deformations from the values of λ and ω_c obtained from the fit. Taking these values to be $\lambda/kT = 0.178$ and $\omega_c = 1.74\times10^{10}$ rad s^{-1}, cf. Table III, one finds that $K = 1.23\times10^{-11}$ N and $\eta = 0.707$ P. The magnitude of K is in agreement with that obtained for nematic liquid crystals [81], whereas the value of η may be less accurate due to the rather large error in the estimation of ω_c. With regard to the composite model, which takes into account both 3D director fluctuations and noncollective molecular diffusion, quantitative information about the rotational diffusion rates and degree of ordering of the lipid molecules can be obtained from fitting the relaxation data. As might be expected, the resulting parameters differ from those obtained from fitting separately the molecular diffusion model (II) to either the orientation dependent or frequency dependent relaxation rates. Compared to the molecular diffusion model (II), the main features of the composite model (V) include a decrease of the rotational diffusion coefficient for off-axial motions $D_\perp$ by approximately an order of magnitude ($\approx 5\times10^6$ s^{-1}), and nearly a threefold increase in the depth of the energy minimum corresponding to $\lambda_j \approx 10-20\ kT$. This would imply an increased molecular ordering $\langle D_{00}^{(2)}(\Omega_{MD})\rangle$ ($\approx 0.8-0.9$) compared to that previously reported ($\approx 0.6-0.7$) [33,44,91], and consequently a decreased segmental ordering $\langle D_{00}^{(2)}(\Omega_{PI})\rangle$, as given by the overall order parameter $S_{\rm CD} = \langle D_{00}^{(2)}(\Omega_{PI})\rangle D_{00}^{(2)}(\Omega_{IM})\langle D_{00}^{(2)}(\Omega_{MD})\rangle$. Neglecting the contribution from small-amplitude director fluctuations, for the composite membrane deformation model (V) the lower limit for the order parameter due to fast segmental motions is estimated to be $S_f^{(2)} \equiv \langle D_{00}^{(2)}(\Omega_{PI})\rangle = 0.4$ for segment C3, with a further decrease along the acyl chain; whereas the order parameter of the slow molecular order fluctuations is $S_s^{(2)} \equiv \langle D_{00}^{(2)}(\Omega_{MN})\rangle\langle D_{00}^{(2)}(\Omega_{ND})\rangle \approx \langle D_{00}^{(2)}(\Omega_{MN})\rangle = 0.9$. The above would suggest that the ^{2}H NMR relaxation of lipid bilayers in the MHz range is governed primarily by collective excitations together with effective axial rotations of the acyl chains.

Another interesting aspect is that the relative contributions from collective and noncollective motions to the nuclear spin relaxation have been found to be comparable in the mid-MHz range. The validity of the present conclusions, however, may be influenced by the fact that the orientational anisotropy of the relaxation rates and frequency dispersion were in fact measured for different samples, i.e., DMPC-d_{54} in the L_α phase versus vesicles of DMPC with specifically ^{2}H-labeled acyl chains. Curvature effects in vesicles may result in slightly different values of the structural parameters [13,92], such as molecular diffusion and bilayer elasticity coefficients. Therefore, the need for obtaining a more comprehensive body of relaxation data for a single lipid system in the L_α phase still remains. Information about transverse relaxation rates [29] could be useful in distinguishing slower motions such as vesicle tumbling [39] or lipid lateral diffusion [93] from collective and noncollective motions. Zero-frequency spectral densities corresponding to the relatively long vesicle tumbling or lateral diffusion correlation times should yield much larger contributions to the transverse relaxation than molecular reorientations or collective fluctuations, which could help separate the motions occurring on different time scales. Alternatively, additional low-frequency relaxation data measured for specific positions in the acyl chain within the kHz range may provide experimental evidence for different regimes of membrane couplings [77,78].

Previous work [16,27,33,43,44] has attempted to identify whether a single predominant motional contribution can explain the R_{1Z} relaxation rates for lipid bilayers in the liquid-crystalline state. However, the results of the present work show that the behavior of the relaxation rates of lipid bilayers as a function of sample orientation and frequency most probably cannot be described to a high degree of accuracy by a simple model accounting for only segmental, molecular, or collective motions. A composite membrane deformation model has been considered herein yielding an expression for the spectral density that contains, in the small-amplitude approximation for collective fluctuations, the sum of the molecular and collective spectral densities, as well as a cross-term that takes into account the combined effect of both noncollective molecular motions and small-amplitude director fluctuations. The ability of the model to describe simultaneously the orientation and frequency dependent R_{1Z} and R_{1Q} relaxation rates means that over the frequency range considered, the ^{2}H NMR relaxation may be governed in general by a composite motional process and not by a single type of motion. This, in turn, increases the complexity of theoretical models and the number of fitting parameters. These findings suggest a new dynamical membrane model in which the phospholipids are effectively tethered to the aqueous interface, with the bilayer interior having a microviscosity due to segmental motions of the acyl chains comparable to that of liquid hydrocarbons. Rotational diffusion of the flexible phospholipid molecules involving segments close to the aqueous interface is accompanied by appreciable chain entanglement deeper in the bilayer interior. The molecular and segmental motions are superimposed upon nematic-type deformations of the entire bilayer, with relatively small wavelengths of excitations ranging between the segmental dimensions and the bilayer thickness or interlamellar separation. Such composite order fluctuations account for both the orientational anisotropy and frequency dependence of the ^{2}H spin relaxation within the MHz range of frequencies, and constitute a new framework for analysis of the dynamics of lipid bilayers and membrane constituents.

ACKNOWLEDGMENTS

The work was supported by grants from the U.S. National Science Foundation, the U.S. National Institutes of Health, and the Swedish Natural Science Research Council. We thank Constantin Job for excellent assistance with the NMR instrumentation, and Regitze R. Vold for helpful discussions.

[1] M. Bloom, E. Evans, and O. G. Mouritsen, Q. Rev. Biophys. **24**, 293 (1991).
[2] R. Zhang, R. M. Suter, and J. F. Nagle, Phys. Rev. E **50**, 5047 (1994).
[3] J. F. Nagle, R. Zhang, S. Tristram-Nagle, W. Sun, and H. Petrache, Biophys. J. **70**, 1419 (1996).
[4] M. F. Brown, in *Biological Membranes. A Molecular Perspective from Computation and Experiment*, edited by K. M. Merz and B. Roux (Birkhäuser, Boston, 1996), p. 175.
[5] Abbreviations used: 2D, two-dimensional; 3D, three-dimensional; EFG, electric field gradient; DLPC-d_{46}, 1,2-diperdeuteriolauroyl-*sn*-glycero-3-phosphocholine; DMPC, 1,2-dimyristoyl-*sn*-glycero-3-phosphocholine; DMPC-d_{54}, 1,2-diperdeuteriomyristoyl-*sn*-glycero-3-phosphocholine; lab, laboratory frame; MD, molecular dynamics; NMR, nuclear magnetic resonance; PAS, principal axis system; POPC-d_{31}, 1-perdeuteriopalmitoyl-2-oleoyl-*sn*-glycero-3-phosphocholine.
[6] M. Bloom, C. Morrison, E. Sternin, and J. L. Thewalt, in *Pulsed Magnetic Resonance: NMR, ESR, and Optics. A Recognition of E. L. Hahn*, edited by D. M. S. Bagguley (Clarendon Press, Oxford, 1992), p. 274.
[7] N. Bloembergen, E. M. Purcell, and R. V. Pound, Phys. Rev. **73**, 679 (1948).
[8] A. G. Redfield, Adv. Magn. Reson. **1**, 1 (1965).
[9] A. Abragam, *The Principles of Nuclear Magnetism* (Oxford University Press, London, 1961).
[10] R. R. Vold, in *Nuclear Magnetic Resonance of Liquid Crystals*, edited by J. W. Emsley (D. Reidel Publishing Company, Dordrecht, 1985), p. 253.
[11] R. R. Vold, in *Nuclear Magnetic Resonance Probes of Molecular Dynamics*, edited by R. Tycko (Kluwer, Dordrecht, 1994), Vol. 8, p. 27.
[12] A. Seelig and J. Seelig, Biochemistry **13**, 4839 (1974).
[13] D. F. Bocian and S. I. Chan, Annu. Rev. Phys. Chem. **29**, 307 (1978).
[14] M. F. Brown, J. Seelig, and U. Häberlen, J. Chem. Phys. **70**, 5045 (1979).
[15] M. F. Brown and J. H. Davis, Chem. Phys. Lett. **79**, 431 (1981).
[16] M. F. Brown, A. A. Ribeiro, and G. D. Williams, Proc. Natl. Acad. Sci. USA **80**, 4325 (1983).
[17] J. H. Davis, Biochim. Biophys. Acta **737**, 117 (1983).
[18] D. J. Siminovitch, M. J. Ruocco, E. T. Olejniczak, S. K. Das Gupta, and R. G. Griffin, Chem. Phys. Lett. **119**, 251 (1985).
[19] J.-M. Bonmatin, I. C. P. Smith, H. C. Jarrell, and D. J. Siminovitch, J. Am. Chem. Soc. **110**, 8693 (1988).
[20] H. C. Jarrell, I. C. P. Smith, P. A. Jovall, H. H. Mantsch, and D. J. Siminovitch, J. Chem. Phys. **88**, 1260 (1988).
[21] E. Rommel, F. Noack, P. Meier, and G. Kothe, J. Phys. Chem. **92**, 2981 (1988).
[22] D. J. Siminovitch, M. J. Ruocco, E. T. Olejniczak, S. K. Das Gupta, and R. G. Griffin, Biophys. J. **54**, 373 (1988).
[23] J. B. Speyer, R. T. Weber, S. K. Das Gupta, and R. G. Griffin, Biochemistry **28**, 9569 (1989).
[24] M. Auger, D. Carrier, I. C. P. Smith, and H. C. Jarrell, J. Am. Chem. Soc. **112**, 1373 (1990).
[25] T. M. Bayerl and M. Bloom, Biophys. J. **58**, 357 (1990).
[26] J.-M. Bonmatin, I. C. P. Smith, H. C. Jarrell, and D. J. Siminovitch, J. Am. Chem. Soc. **112**, 1697 (1990).
[27] M. F. Brown, A. Salmon, U. Henriksson, and O. Söderman, Mol. Phys. **69**, 379 (1990).
[28] C. Mayer, G. Gröbner, K. Müller, K. Weisz, and G. Kothe, Chem. Phys. Lett. **165**, 155 (1990).
[29] J. Stohrer, G. Gröbner, D. Reimer, K. Weisz, C. Mayer, and G. Kothe, J. Chem. Phys. **95**, 672 (1991).
[30] K. Weisz, G. Gröbner, C. Mayer, J. Stohrer, and G. Kothe, Biochemistry **31**, 1100 (1992).
[31] T. Köchy and T. M. Bayerl, Phys. Rev. E **47**, 2109 (1993).
[32] R. L. Thurmond, G. Lindblom, and M. F. Brown, Biochemistry **32**, 5394 (1993).
[33] T. P. Trouard, T. M. Alam, and M. F. Brown, J. Chem. Phys. **101**, 5229 (1994).
[34] C. Morrison and M. Bloom, J. Chem. Phys. **101**, 749 (1994).
[35] C. Dolainsky, M. Unger, M. Bloom, and T. M. Bayerl, Phys. Rev. E **51**, 4743 (1995).
[36] M. F. Brown and S. I. Chan, in *Encyclopedia of Nuclear Magnetic Resonance*, edited by D. M. Grant and R. K. Harris (Wiley, New York, 1996), Vol. 2, p. 871.
[37] A. A. Nevzorov, T. P. Trouard, and M. F. Brown, Phys. Rev. E **55**, 3276 (1997).
[38] M. F. Brown, J. Magn. Reson. **35**, 203 (1979).
[39] B. Halle, J. Phys. Chem. **95**, 6724 (1991).
[40] C. Zannoni, Mol. Phys. **38**, 1813 (1979).
[41] T. M. Barbara, R. R. Vold, and R. L. Vold, J. Chem. Phys. **79**, 6338 (1983).
[42] C. Morrison and M. Bloom, J. Magn. Reson., Ser. A **103**, 1 (1993).
[43] M. F. Brown, J. Chem. Phys. **77**, 1576 (1982).
[44] A. A. Nevzorov and M. F. Brown, J. Chem. Phys. **107**, 10288 (1997).
[45] T. P. Trouard, dissertation University of Virginia, 1992 (unpublished).
[46] B. Halle, P.-O. Quist, and I. Furó, Phys. Rev. A **45**, 3763 (1992).
[47] P.-O. Quist, J. Phys. Chem. **100**, 4976 (1996).
[48] H. W. Spiess, in *NMR Basic Principles and Progress*, edited by P. Diehl, E. Fluck, and R. Kosfeld (Springer-Verlag, Heidelberg, 1978), Vol. 15, p. 55.
[49] M. E. Rose, *Elementary Theory of Angular Momentum* (Wiley, New York, 1957).
[50] D. M. Brink and G. R. Satchler, *Angular Momentum* (Oxford University Press, London, 1968).
[51] T. P. Trouard, T. M. Alam, J. Zajicek, and M. F. Brown, Chem. Phys. Lett. **189**, 67 (1992).
[52] D. A. Torchia and A. Szabo, J. Magn. Reson. **49**, 107 (1982).
[53] R. J. Wittebort, E. T. Olejniczak, and R. G. Griffin, J. Chem. Phys. **86**, 5411 (1987).
[54] A. Ferrarini, P. L. Nordio, G. J. Moro, R. H. Crepeau, and J. H. Freed, J. Chem. Phys. **91**, 5707 (1989).
[55] R. Cassol, A. Ferrarini, and P. L. Nordio, J. Phys. Chem. **97**, 2933 (1993).
[56] D. J. Schneider and J. H. Freed, Adv. Chem. Phys. **73**, 387 (1989).
[57] R. W. Pastor, R. M. Venable, M. Karplus, and A. Szabo, J. Chem. Phys. **89**, 1112 (1988).
[58] H. De Loof, S. C. Harvey, J. P. Segrest, and R. W. Pastor, Biochemistry **30**, 2099 (1991).
[59] R. M. Venable, Y. Zhang, B. J. Hardy, and R. W. Pastor, Science **262**, 223 (1993).
[60] H. E. Alper, D. Bassolino-Klimas, and T. R. Stouch, J. Chem. Phys. **99**, 5547 (1993).

[61] S.-W. Chiu, M. Clark, V. Balaji, S. Subramaniam, H. L. Scott, and E. Jakobsson, Biophys. J. **69**, 1230 (1995).
[62] K. Tu, D. J. Tobias, and M. L. Klein, Biophys. J. **69**, 2558 (1995).
[63] R. W. Pastor and S. E. Feller, in *Biological Membranes. A Molecular Perspective from Computation and Experiment*, edited by K. M. Merz and B. Roux (Birkhäuser, Boston, 1996), p. 3.
[64] R. Blinc, M. Luzar, M. Vilfan, and M. Burgar, J. Chem. Phys. **63**, 3445 (1975).
[65] J. A. Marqusee, M. Warner, and K. A. Dill, J. Chem. Phys. **81**, 6404 (1984).
[66] P. Pincus, Solid State Commun. **7**, 415 (1969).
[67] P. Ukleja, J. Pirs, and J. W. Doane, Phys. Rev. A **14**, 414 (1976).
[68] M. F. Brown, J. F. Ellena, C. Trindle, and G. D. Williams, J. Chem. Phys. **84**, 465 (1986).
[69] R. Blinc, in *NMR Basic Principles and Progress*, edited by P. Diehl, E. Fluck, and R. Kosfeld (Springer-Verlag, Heidelberg, 1976), Vol. 13, p. 97.
[70] R. L. Vold, R. R. Vold, and M. Warner, J. Chem. Soc., Faraday Trans. 2 **84**, 997 (1988).
[71] M. F. Brown and O. Söderman, Chem. Phys. Lett. **167**, 158 (1990).
[72] P. L. Nordio and U. Segre, in *The Molecular Physics of Liquid Crystals*, edited by G. R. Luckhurst and G. W. Gray (Academic Press, New York, 1979), p. 411.
[73] A. Szabo, J. Chem. Phys. **81**, 150 (1984).
[74] C. Zannoni, in *Nuclear Magnetic Resonance of Liquid Crystals*, edited by J. W. Emsley (D. Reidel Publishing Company, Dordrecht, 1985), p. 1.
[75] G. D. Williams, J. M. Beach, S. W. Dodd, and M. F. Brown, J. Am. Chem. Soc. **107**, 6868 (1985).
[76] A. Salmon, S. W. Dodd, G. D. Williams, J. M. Beach, and M. F. Brown, J. Am. Chem. Soc. **109**, 2600 (1987).
[77] B. Halle, Phys. Rev. E **50**, R2415 (1994).
[78] B. Halle and S. Gustafsson, Phys. Rev. E **56**, 690 (1997).
[79] T. E. Faber, Proc. R. Soc. London, Ser. A **353**, 247 (1977).
[80] J. H. Freed, J. Chem. Phys. **66**, 4183 (1977).
[81] R. Y. Dong, *Nuclear Magnetic Resonance of Liquid Crystals* (Springer-Verlag, New York, 1994).
[82] J. T. Mason, A. V. Broccoli, and C. H. Huang, Anal. Biochem. **113**, 96 (1981).
[83] S. W. Dodd, thesis (University of Virginia, 1987).
[84] H. C. Jarrell, P. A. Jovall, J. B. Giziewicz, L. A. Turner, and I. C. P. Smith, Biochemistry **26**, 1805 (1987).
[85] J. H. Davis, K. R. Jeffrey, M. Bloom, M. I. Valic, and T. P. Higgs, Chem. Phys. Lett. **44**, 390 (1976).
[86] M. Bloom, J. H. Davis, and M. I. Valic, Can. J. Phys. **58**, 1510 (1980).
[87] R. R. Vold and G. Bodenhausen, J. Magn. Reson. **39**, 363 (1980).
[88] S. Wimperis, J. Magn. Reson. **86**, 46 (1990).
[89] G. L. Hoatson, J. Magn. Reson. **94**, 152 (1991).
[90] J. F. Nagle, J. Chem. Phys. **103**, 1720 (1995).
[91] M. F. Brown, J. Chem. Phys. **80**, 2808 (1984).
[92] Y. I. Parmar, S. R. Wassall, and R. J. Cushley, J. Am. Chem. Soc. **106**, 2434 (1984).
[93] G. Lindblom and G. Orädd, Prog. Nucl. Magn. Reson. Spectrosc. **26**, 483 (1994).
[94] P. R. Bevington, *Data Reduction and Error Analysis for the Physical Sciences* (McGraw-Hill, New York, 1969).